European Journal of Medicinal Chemistry 288 (2025) 117395

Contents lists available at ScienceDirect

European Journal of Medicinal Chemistry

journal homepage: www.elsevier.com/locate/ejmech

Research paper

Design and synthesis of novel thioether analogs as promising antiviral agents: *In vitro* activity against enteroviruses of interest

Hugo Roux [a], Franck Touret [b], Antonio Coluccia [c], Pietro Scio [c], Hawa Sophia Bouzidi [b], Carole di Giorgio [d], Florence Gattacceca [e], Omar Khoumeri [a], Romano Silvestri [c], Patrice Vanelle [a,*], Manon Roche [a,**]

[a] Aix-Marseille Université, CNRS, ICR UMR 7273, PCR, Faculté de Pharmacie, 13005, Marseille, France
[b] Unité des Virus Émergents (UVE: Aix-Marseille Univ, Università di Corsica, IRD 190, Inserm 1207, IRBA), France
[c] Department of Drug Chemistry and Technologies, Laboratory Affiliated with the Institute Pasteur Italy – Cenci Bolognetti Foundation, Sapienza University of Rome, Italy
[d] Aix-Marseille Université, Avignon Université, CNRS, IRD, IMBE, Faculty of Pharmacy, Service of Environmental Mutagenesis, Marseille, France
[e] Aix-Marseille Université, COMPO INRIA–CRCM-INSERM-U1068, CNRS UMR7258, Marseille, France

ARTICLE INFO

Keywords:
Enterovirus
Capsid binder
Broad-spectrum
Structure-activity relationships
Fused bicycles
Heterocyclic compounds

ABSTRACT

The *Enterovirus* genus contains two major subgroups: rhinovirus (RV) species A-C and enterovirus (EV) ones A-D. While RV only infects the respiratory system, the EV can cause a wide variety of diseases, ranging from non-specific febrile illness to severe neurologic complications. To date, no curative treatments are commercially available. Our research team had recently developed EV-A71 inhibitors. To improve their activity and broaden their spectrum, we performed optimization of the structure following an iterative cycle of chemical modulations. As a result, we obtained two broad-spectrum inhibitors with micromolar activity against these 3 types of viruses (**OM1260**: EC_{50} (MRC-5, EV-A71) = 1.15 μM; EC_{50} (RD, EV-A71) = 4.38 μM; EC_{50} (MRC-5, E30) = 0.41 μM; EC_{50} (MRC-5, CVA24) = 1.15 μM; **HR-568**: EC_{50} (MRC-5, EV-A71) = 3.25 μM; EC_{50} (RD, EV-A71) = 1.53 μM; EC_{50} (MRC-5, E30) = 0.40 μM; EC_{50} (MRC-5, CVA24) = 1.22 μM). Docking studies shed light on structure-activity relationships, while time-of-drug addition assays confirmed their intervention during the early step of viral replication. Eventually, some pharmacokinetic modelling has been carried out to evaluate their druggability. All these results showed that **OM1260** and **HR-568** are promising candidates for further development.

1. Introduction

The *Enterovirus* genus of the *Picornaviridæ* family contains many important human pathogens. It is composed of 7 species, namely 4 enterovirus species (EV-A, -B, –C, -D) and 3 human rhinovirus species (RV-A, -B, –C). Some types of virus can be associated with severe and specific clinical manifestations for immunocompromised or pediatric patients. EVs are ubiquitous, with a diversity of species and variants among continental regions [1]. EV-B is the most detected species worldwide, while EV-A has been mainly observed in Pacific Asia in contrast to North America, where most of the infections reported have been caused by EV-D. In addition, new viral variants have emerged these last decades, such as enterovirus-A71 (EV-A71) and enterovirus-D68 (EV-D68), causing outbreaks associated with more severe disease manifestations than previously described [2–4]. Moreover, even if the number of infections due to EV decreased during and shortly after the (SARS-Cov2) lockdown, numerous enterovirus outbreaks were once again detected. Indeed, EV-D outbreaks were detected as early as 2021 [5]. Eventually, as a greater sensitivity in young children was identified in CV-B5 and E11 infections, there is a need to develop a broad-spectrum enterovirus inhibitor to address their growing threat [6].

In our previous projects to design some broad-spectrum anti-enteroviral compounds, we developed 210 molecules inhibiting rhinoviruses or EV-A71 [7–12]. From the last works, we observe that the

* Corresponding author.
** Corresponding author.
E-mail addresses: hugo.roux@univ-amu.fr (H. Roux), franck.touret@univ-amu.fr (F. Touret), antonio.coluccia@uniroma1.it (A. Coluccia), pietro.scio@uniroma1.it (P. Scio), hawa-sophia.BOUZIDI@univ-amu.fr (H.S. Bouzidi), carole.di-giorgio@univ-amu.fr (C. di Giorgio), florence.gattacceca@univ-amu.fr (F. Gattacceca), omar.khoumeri@univ-amu.fr (O. Khoumeri), romano.silvestri@uniroma1.it (R. Silvestri), patrice.vanelle@univ-amu.fr (P. Vanelle), manon.roche@univ-amu.fr (M. Roche).

https://doi.org/10.1016/j.ejmech.2025.117395
Received 27 December 2024; Received in revised form 3 February 2025; Accepted 11 February 2025
Available online 14 February 2025
0223-5234/© 2025 The Authors. Published by Elsevier Masson SAS. This is an open access article under the CC BY license (http://creativecommons.org/licenses/by/4.0/).

thioether linker improved EV growth inhibition. This is the first compound series using sulfur as a heteroatom in the linker with 4 aromatic cycles for EV capsid binders [13–16]. Four molecules were defined as potent inhibitors on MRC-5 against EV-A71 [Table 1]. **AB112** and **AB113** were the most promising candidates against EV-A71, considering two cell lines: MRC-5 and rhabomyosarcoma (RD).

To analyze the interactions of AB113, our most promising compound, with the hydrophobic pocket, we modulated configurations of benzyl alcohol on the toe-end side and nitrogen of the pore aromatic cycle [Fig. 1]. Then, to combine the properties of AB109 and AB113 derivatives, we decided to modulate the toe-end side with fused cycles. Likewise, new five- or six-membered aromatic heterocycles were evaluated as pore pharmacophores.

To access a preclinical lead from our compounds, some *in silico* predictions of pharmacokinetic parameters were performed. Moreover, some antiviral assays on other enteroviruses are considered to evaluate the spectrum of activity of our compounds and move toward broad-spectrum enterovirus inhibitors design. In addition to the EV-A71, the E30 has been selected for its prevalence, particularly in Europe, while CVA24 is known for its variant causing acute hemorrhagic conjunctivitis. A time-of-addition assay (TOA) was carried out to confirm the action of our compounds when the virus enters the host cell.

2. Results

2.1. Chemistry

2.1.1. Synthesis pathways

Twenty-two compounds were synthesized according to the synthesis pathways detailed in Scheme 1, already reported in our previous works [17]. Functionalization of both toe-end and pore sides was performed using various boronic acids.

As presented before, we change the substitution of the toe-end alcohol function and the nitrogen position in the pore side aromatic cycle for **AB113** optimization. Moreover, we also decided to gather both **AB113** and **AB109** toe-end pharmacophores to enhance the activity of our newly synthesized compounds. Consequently, we modulated the toe-end side with fused aromatic cycles or aromatic heterocycles. Likewise, we also changed the pore triazole pharmacophore, selecting five-membered heterocycles, namely *N*-benzyl or *N*-methylpyrazole, and 3,5-dimethylisoxazole, or six-membered heterocycles, namely 3- or 4-*N*-dimethylaniline. Preliminary docking assays predicted that *meta* dimethylaniline at the pore side could have an effective binding of bicycle derivatives (compounds **5d** and **5e**). Thus, the compounds **5a-e** were also synthesized with this procedure. At last, cycle B was also modulated between aromatic heterocycles (phenyl, pyridine, 2-thiohydantoin).

The Supplementary Materials contain all the 1H NMR, and 13C NMR spectra, HRMS-ESI, and chemical purity data of target compounds.

Table 1
The activity of thioether derivatives against enterovirus EV-A71.

Compound	Structure	EC_{50} (MRC-5, μM)	EC_{50} (RD, μM)
Vapendavir	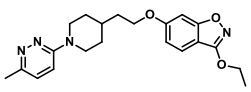	0.36 ± 1.61	0.56 ± 1.63
AB109	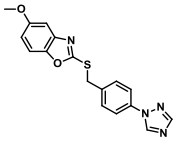	1.67 ± 2.23	28.53 ± 2.23[a]
HR266	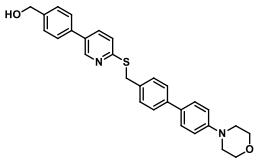	6.38	19.71 ± 2.33
AB112	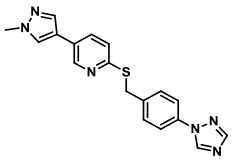	0.57 ± 2.5	4.38 ± 2.16
AB113	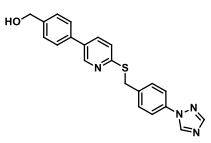	0.29 ± 2.35	1.66 ± 2.18

[a] Cytotoxicity detected: CC50 (RD) = 22.10 μM.

2.1.2. General Procedure

We have chosen to keep the synthesis strategy previously described to obtain the desired compounds by considering the difficulty of synthesis, the economy of atoms, and the synthesis steps [7]. Most of boronic acids used in these pathways are commonly used [17].

The functionalization of the pore side was performed by Suzuki-Miyaura cross-coupling, with the highly reactive catalyst **Pd(dppf)Cl_2**, to lead to derivatives **1a-e**, in yields of between 76 % and 94 % (Scheme 1, route a). A reduction with sodium borohydride **$NaBH_4$** led to benzyl alcohol derivatives **2a-f**, with yields of 93 % and 100 %. Then a chlorination with thionyl chloride **$SOCl_2$** was performed to obtain chloro derivatives **3a-f** in yield between 85 % and 97 % (Scheme 1, routes b and c). To prepare derivatives **4a-f, h**, the chloro derivatives **3a-f** were coupled with 3-bromo-6-mercaptopyridine (**BrPhSh**) or 4-bromothiophenol (**BrPySH**), providing yields ranging from 73 % to 100 % (Scheme 1, routes d). Eventually, final products **5a-n** were synthesized using a Suzuki-Miyaura cross-coupling, catalyzed with **Pd(dppf)Cl_2** (Scheme 1, routes e). This step had yields from 40 % to 99 %.

A bimolecular nucleophilic substitution between **3f** and **(*Z*)-5-((1*H*-indol-3-yl)methylene)-2-thiohydantoin** was performed with yields of 50 % to synthesize derivative **6** (Scheme 2) [7].

2.1.3. Pyrimidine functionalization

The functionalization with appropriate pyrimidine was performed using a procedure already reported (Scheme 3) [7].

This strategy led to intermediate **7**, which allows us to functionalize the pore side easily. 6 final products were synthesized in two steps from the bromo derivative **7**. The pore functionalization for compounds **8a-f** was made by Suzuki-Miyaura cross-coupling, catalyzed with Pd(dppf)Cl2, with yields ranging from 73 % to 93 %. Eventually, a reduction of compounds **8a-f** with NaBH4 led to final compounds **9a-f** with yields between 24 % and 100 %.

2.2. In vitro biological assays

To determine the activity of our new compounds against enteroviruses, we performed our standardized *in vitro* RNA yield-reduction antiviral assays [18]. These assays allowed us to estimate their antiviral activity through their half-maximal effective concentration (EC_{50}). We used two different cell lines: Rhabdomyosarcoma (RD) and Medical Research Council cell strain 5 (MRC-5). By assessing antiviral activity in two different cell lines, we reduce the risk of cell-specific activity and increase the confidence of our results [19]. Half-maximal cytotoxic concentration (CC50) was also measured in parallel in compound-treated uninfected cells.

To determine the most effective inhibitor among our synthesized compounds, first, we performed assays with an EV-A71 strain. Then, we

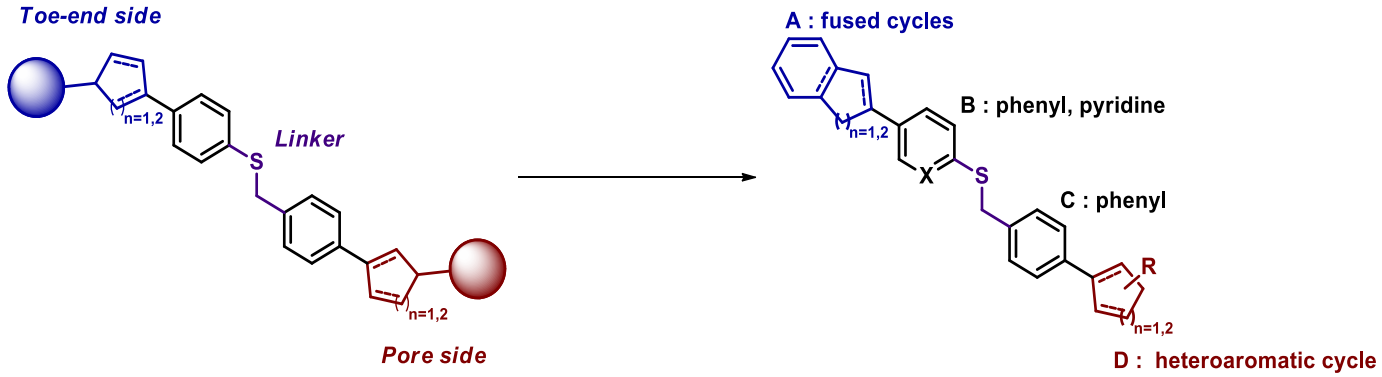

Fig. 1. Combination of AB109 bicycles with AB113 derivatives, introducing cycle's nomenclatures and hydrophobic pocket sides.

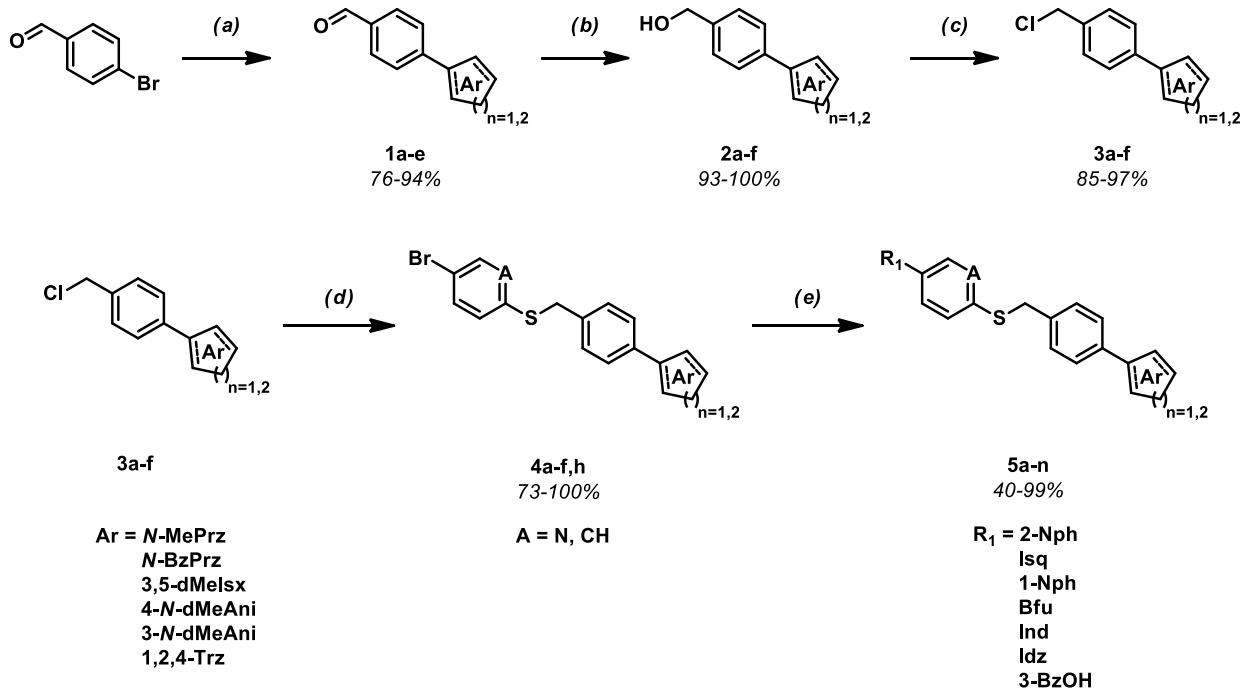

Scheme 1. Procedure A for the Synthesis of the toe-end modulated AB113 analogs and bicycle derivatives [a].[a]Reagents and conditions: (*a*) $ArB(OH)_2$, $Pd(dppf)Cl_2$, K_2CO_3, Dioxane:H_2O (4:1), 80 °C, N_2, p; (*b*) $NaBH_4$, DCM:MeOH (1:1), 0 °C to rt, 2 h, N_2, p; (*c*) $SOCl_2$, DCM or DMF, 0 °C to rt, 3 h, N_2; (*d*) **BrPhSh** or **BrPySH**, K_2CO_3, ACN, 80 °C, N_2, p; (*e*) $ArB(OH)_2$, $Pd(dppf)Cl_2$, K_2CO_3, Dioxane:H_2O (4:1), 80 °C, N_2, p; (*f*) **IndThd**, K_2CO_3, ACN, 80 °C, N_2, p.

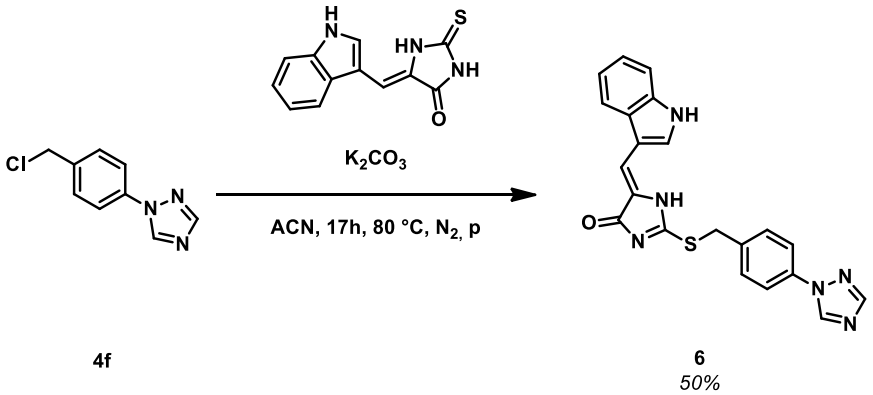

Scheme 2. General Procedure for the synthesis derivative 6.

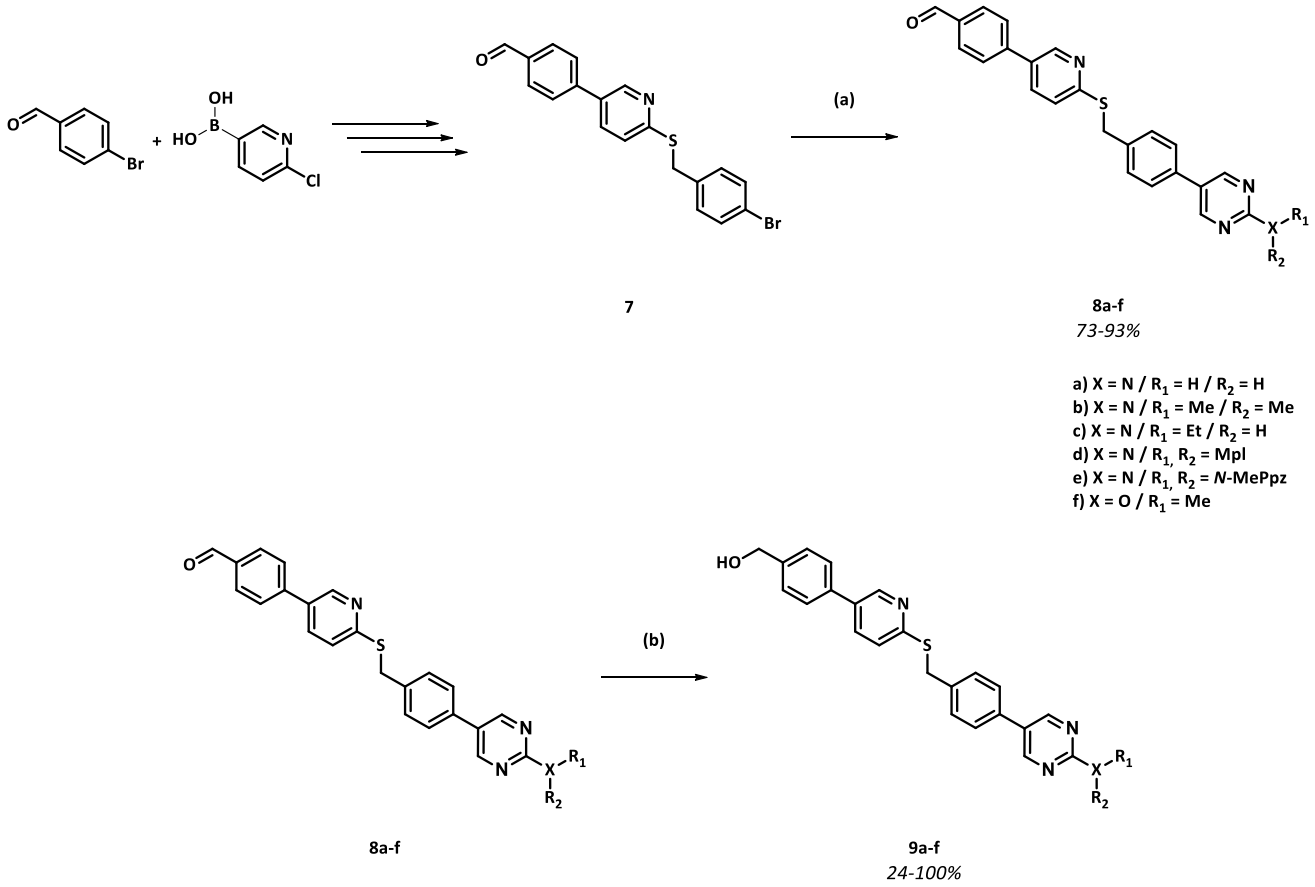

Scheme 3. Pyrimidine pore functionalization synthesis pathway [a]. [a]Reagents and conditions: (a) $ArB(OH)_2$, $Pd(Dppf)Cl_2$, K_2CO_3, Dioxane:H_2O (4:1), 80 °C, N_2, p; (b) $NaBH_4$, DCM:MeOH (1:1), rt, 2 h, N_2, p.

explored the broad-spectrum activity against E30 and CV-A24, respectively, from EV species B and C. Vapendavir, a capsid binder, was used as a reference compound in our assays [20]. We chose MRC-5 and RD cells line as they were already used in other antienteroviral works against EV-A71 for both and against E30 and CV-A24 for MRC-5 [7,21–23].

2.2.1. Evaluation of AB113 analogs

From the previous works, two molecules were defined as promising candidates: **AB112** and **AB113**. However, some interactions remain unclear. Indeed, the orientation of methylalcohol in the toe-end was not evaluated yet, as well as the role of nitrogen atoms of the pore side aromatic cycle, in the activity enhancement. Consequently, to assess **AB113** structure optimization, we first synthesized a derivative with a toe-end *meta*-substituted methylalcohol instead of *para*-substituted. Moreover, we decided to modulate the pore side, introducing an aminopyrimidine ring instead of a triazole (to retain the number of nitrogen atoms) and using various substitutions on 2-aminopyrimidine. Antiviral assays' results are presented in Table 2.

The *in vitro* biological assays clarified that the para methanol substituent at the toe-end was crucial because its shifting to the *meta* position markedly affected the potency. In the same way, the triazole ring at the pore side was crucial too. Indeed, the introduction of 2-aminopyrimidine affected potency, and substituted 2-aminopyridine completely abrogated the antiviral activity.

2.2.2. Bicycle pharmacomodulation at the toe-end side

Considering the pharmacophoric elements of **AB109** and **AB113** compounds, we modulated both the toe-end and pore sides. Thus, we replaced the benzyl alcohol of **AB113** with various fused aromatic bicycles, retaining the other part of the scaffold. Oxygen or nitrogen atoms were inserted in the bicycle rings, trying to retain the alcohol group's capabilities to form hydrogen bond contacts. Activities for each modulation are presented in Table 3.

By comparing the different results on the two cell lines, we were able to identify the most promising inhibitors. **OM1260**, **HR-394**, and **HR-568** were the most effective compounds against EV-A71 [Fig. 2]. **HR-478** has a lower potency on RD cells, while no activity was quantified in MRC-5 cells. Other compounds did not show antiviral activity against EV-A71 in these conditions.

2.2.3. Evaluation of heteroaromatic pharmacophores at the pore side

Having determined the best toe-end functionalization, we also modulated the pore side with five-membered aromatic cycles, as triazole seemed to be the best pharmacophore. Activities for each modulation are presented in Table 4.

Any of the *pore* modulations presented a better activity than triazole derivatives. Indeed, the more the five-membered aromatic heterobicycles are substituted with bulky moieties, the more the steric hindrance seems to decrease the potency of the compound. *N*-methylpyrazole is more effective than dimethylisoxazole, itself being more active than *N*-benzylpyrazole. Loss of activity was observed for *N*-dimethylaniline, for both *meta* and *para* substitution. Six-membered modulation led to loss of activity.

2.2.4. Inhibition of enteroviruses from 3 different species (CVA24, E30, EV-A71)

As our main objective is to synthesize broad-spectrum enterovirus inhibitors, we performed RNA yield-reduction antiviral assays against other types of viruses. Here, we focus on 3 types of viruses, namely EV-A71, E30, and CVA24, included in EV-A, EV-B, and EV-C species

Table 2
In vitro antiviral activity of AB113 derivatives against EV-A71 on MRC-5 and RD cells.[a]

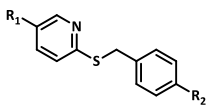

			MRC-5			Rhabdomyosarcoma		
Inhibitors	R1	R2	EC_{50} (μM)[b]	CC_{50} (μM)[c]	SI[d]	EC_{50} (μM)[b]	CC_{50} (μM)[c]	SI[d]
Vapendavir	/	/	0.36 ± 1.61	>20	>55	0.53 ± 1.65	>63	>118
5n	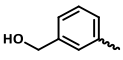		22.01	>40	>1.8	2.78	>40	>14
9a = HR-267	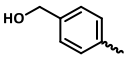	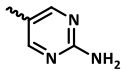	<0.37	>20	>54	24.7	44.66	1.81
9b	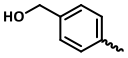	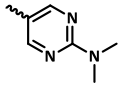	/	/	/	>40	/	/
9f	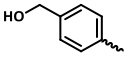	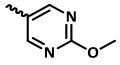	/	/	/	>40	/	/
9d	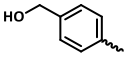	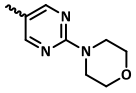	/	/	/	>40	/	/
9e	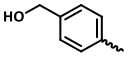	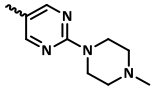	/	/	/	>40	/	/
9c	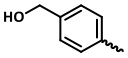	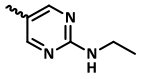	/	/	/	>40	/	/

[a] Values reported as median ± std are from two independent experiments.
[b] EC_{50} = 50 % effective concentration (concentration at which 50 % inhibition of virus-induced cell death is observed).
[c] CC_{50} = 50 % cytotoxic concentration (concentration at which 50 % adverse effect is observed on host cell viability).
[d] SI = selectivity index for EV-A71, SI=CC_{50}/EC_{50}.

[Table 5]. EV-A71 is the main cause of hand-foot-mouth disease, which is circulating in many Asia-Pacific countries. Moreover, severe infections were responsible for neurologic conditions as well as E30 ones, while a variant of CVA24 causes acute hemorrhagic conjunctivitis.

2.2.5. Early step inhibition by HR-568

To gain a better understanding of the **HR-568** mode of action, we performed TOA using the same conditions as the EC_{50} determination. To clearly distinguish the difference in inhibition, we performed the experiment, higher than the EC_{50}, at 10 μM in RD cells. We tested 4 different times, 1 h before infection, at the same time (0), 1 and 4 h after infection. We used two complementary readouts: viral RNA copy number in the supernatant and % viral inhibition [Fig. 3].

The experiment was conducted using the same conditions as the EC_{50} determination. Data presented are from 3 or 6 technical replicates, and error bars show mean ± s.d.

First, 1-h pre-incubation is the condition with the greatest reduction (1.5 log compared to VC) and over 90 % inhibition. The standard condition gives a 1.25 log reduction and over 90 % inhibition. At 1-h post-infection, we observed a further slight decrease in reduction to 1.14 log, but still over 90 % inhibition. At 4 h post-infection we observe the greatest inhibition decrease with only 0.7 log, translating into less than 90 % inhibition. These results seem to indicate that HR-568, which is a capsid binder, does have an antiviral effect on the early phase of viral replication. Given that, in our assay, there are several replication cycles, and our reduction in antiviral activity is not total, we cannot exclude a minor antiviral activity in the late phase of viral replication.

2.3. Evaluation of mutagenic activity of active compounds (HR-267, HR-394, HR-568, OM1260)

To completely evaluate the toxicity of our compounds, in addition to simple cytotoxicity ones, we performed mutagenic assays on Chinese Hamster Ovary (CHO) cells. This is why, firstly, we assess the cytotoxicity of our most promising compounds. Then, we evaluate the clastogenic and aneugenic power of these compounds, with or without metabolic activation.

2.3.1. Cytotoxicity evaluation of our most promising compounds

To check every pre-clinical criterion, we didn't only evaluate the activity of our compound but also their cytotoxicity. Half-maximal cytotoxic concentration (CC_{50}) on MRC-5 and RD cells for all synthesized compounds are represented in Table 2, Table 3, or Table 4. Rh most promising compounds were also assayed to evaluate CC_{50} on CHO cells. Results are presented in Table 6. Most of them have a selective index superior of 10. Only **HR-267** or **OM1260** in RD cells have respectively 1.81 and 6.62 for selective index. Moreover, all of them have a CC_{50} superior to 20 μM on every cell line. On MRC-5, the upper limit of measure is too low to identify the precise CC_{50}. On RD cells, our most promising compounds can be ranged with a CC_{50} from 23.51 μM to 96.29 μM. On the contrary, on CHO, all values are between 30 and 45 μM. Regarding the effect on the cell viability of the CHO cells, no

Table 3
In vitro antiviral activity of toe-end modulation against EV-A71 on MRC-5 and RD cells.[a]

	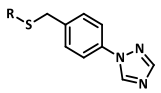	MRC-5			Rhabdomyosarcoma		
Inhibitors	R	EC_{50} (μM)[b]	CC_{50} (μM)[c]	SI[d]	EC_{50} (μM)[b]	CC_{50} (μM)[c]	SI[d]
Vapendavir	/	0.36 ± 1.61	>20	>55	0.53 ± 1.65	>63	>118
5j = OM1260	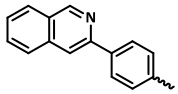	1.15 ± 0.62	>40	>25	4.30 ± 1.29	30.54 ± 4.95	7.10
5h	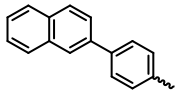	/	/	/	>40	/	/
5i	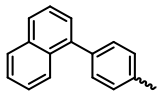	/	/	/	>40	/	/
5k	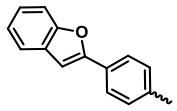	/	/	/	>40	/	/
5l	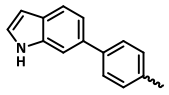	/	/	/	>40	/	/
5m	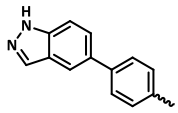	/	/	/	>40	/	/
5g	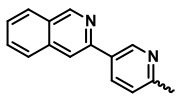	>20	/	/	22.10 ± 1.76	>40	>1.8
5f = HR-568	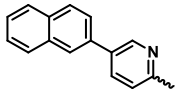	3.25 ± 0.12	>40	>12	1.86 ± 0.47	23.51	12.5
6 = HR-394	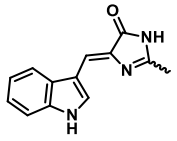	>40	/	/	4.65	96.29	20.7

[a] Values reported as median ± std are from two independent experiments.
[b] EC_{50} = 50 % effective concentration (concentration at which 50 % inhibition of virus-induced cell death is observed).
[c] CC_{50} = 50 % cytotoxic concentration (concentration at which 50 % adverse effect is observed on host cell viability).
[d] SI = selectivity index for EV-A71, SI=CC_{50}/EC_{50}.

interferences should appear in our mutagenicity assays.

2.3.2. Evaluation of clastogenic and aneugenic effects of effective agents

The micronucleus assay protocol was performed as validated by the Organisation for Economic Co-operation and Development [24]. The procedure for assessing mutagenicity has already been described in our previous work [7]. The results are reported in Supplementary Materials Table 1 without S9 mix [Suppl. Table 1A] or with S9 mix [Suppl. Table 1B].

According to these results, none of our promising compounds significantly increased micronucleated cell rates. Consequently, neither **OM1260**, **HR-267**, **HR-394**, nor **HR-568** exerts cytogenetic effects on *in vitro* CHO cell lines or produces metabolites with cytogenetic effects. In these conditions, none of these capsid binders ever became devoid of clastogenic or aneugenic activities.

2.4. Docking studies

All the newly reported compounds were studied by docking experiments to gain more insight into the binding mode and highlight the pharmacophoric interactions. In general, all derivatives shared a consistent binding mode superimposable with the one described for the parent compound **AB113** [7]. Only derivative **HR-394** had an unrelated binding pose.

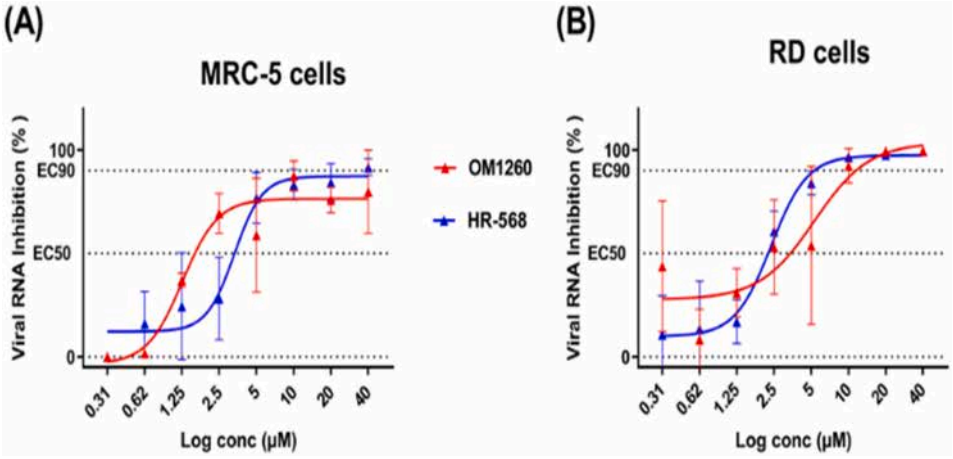

Fig. 2. Dose-response curve reporting the antiviral activity of OM1260/HR-568 against EV-A71. Antiviral activity in A) MRC-5 cells and B) RD cells. Data presented are from three technical replicates, and error bars show mean ± s.d.

Table 4
In vitro antiviral activity of toe-end modulation against EV-A71 on MRC-5 and RD cells.[a]

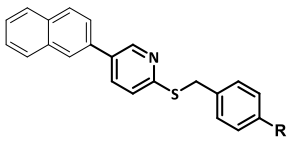

		MRC-5			Rhabdomyosarcoma		
Inhibitors	R	EC_{50} (μM)[b]	CC_{50} (μM)[c]	SI[d]	EC_{50} (μM)[b]	CC_{50} (μM)[c]	SI[d]
Vapendavir	/	0.36 ± 1.61	>20	>55	0.53 ± 1.65	>63	>118
5f = HR-568		3.25 ± 0.12	>40	>12	1.53 ± 0.47	23.51	12.5
5a		22.41	>40	>1.8	11.96	>40	>3.3
5c		>40	/	/	22.28	>40	>1.8
5b	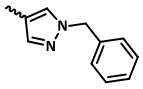	/	/	/	>40	/	/
5d	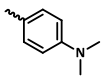	/	/	/	>40	/	/
5e	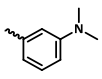	/	/	/	>40	/	/

[a] Values reported as median ± std are from two independent experiments.
[b] EC_{50} = 50 % effective concentration (concentration at which 50 % inhibition of virus-induced cell death is observed).
[c] CC_{50} = 50 % cytotoxic concentration (concentration at which 50 % adverse effect is observed on host cell viability).
[d] SI = selectivity index for EV-A71, SI=CC_{50}/EC_{50}.

The inspections of the proposed binding poses highlighted a series of crucial interactions. The triazole ring at the pore side was involved in hydrophobic interactions with F233, F137, V190, and P177 residues (**5g**, **HR-568**, **OM1260**) [Fig. 4, Suppl. Fig. 1]. Likewise, pyrimidine moiety is involved in the same interactions (**HR-267**). The introduction of bulkier moieties instead of the triazole (**9b**, **9c**, **9d**, **9e**, **9f**) negatively affected the binding mode mainly for steric clashes (Data not shown).

H-bonds are also reported as yellow dot lines while stacking/aromatic contacts are depicted as black dot lines.

The scaffold of the compounds (ring C-linker-ring B) had extensive stabilization. In particular, the phenyl ring C was involved in aromatic interactions with F155 and F135, linker atoms were stabilized by V192 and I111, and ring B (phenyl/pyridine) had aromatic contacts with Y201 [Fig. 4].

The introduction of a bicycle instead of ring A did not affect the binding mode. For 6-member bicycle rings (**OM1260**, **HR-568**), a large hydrophobic interaction with W203 and I113 was observed [Fig. 4].

Worthily, derivative **5n**, with the alcohol moiety in *meta*, did not show differences compared to the parent compound; also, the H-bond with D112 was conserved [Suppl. Fig. 2].

Table 5
In vitro evaluation of pan-EV activities of most promising compounds on MRC-5 cells.[a]

Compound	EC_{50} (EV-A71)[b]	EC_{50} (E30)[b]	EC_{50} (CVA24)[b]	CC_{50}[c]	SI (EV-A71)[d]	SI (E30)[d]	SI (CVA24)[d]
AB113	0.29 ± 2.35	>40	23.25	>40	>181	/	>1.7
OM1260 = 5j	1.15 ± 0.62	0.41	1.22	>40	>25	>100	>32
HR-568 = 5f	3.25 ± 0.12	0.40	0.99	>40	>12	>100	>40

[a] Values reported as median ± std are from two independent experiments.
[b] EC_{50} = 50 % effective concentration (concentration at which 50 % inhibition of virus-induced cell death is observed).
[c] CC_{50} = 50 % cytotoxic concentration (concentration at which 50 % adverse effect is observed on host cell viability).
[d] SI = selectivity index for several viruses (EV-A71, E30, CVA24), SI=CC_{50}/EC_{50}.

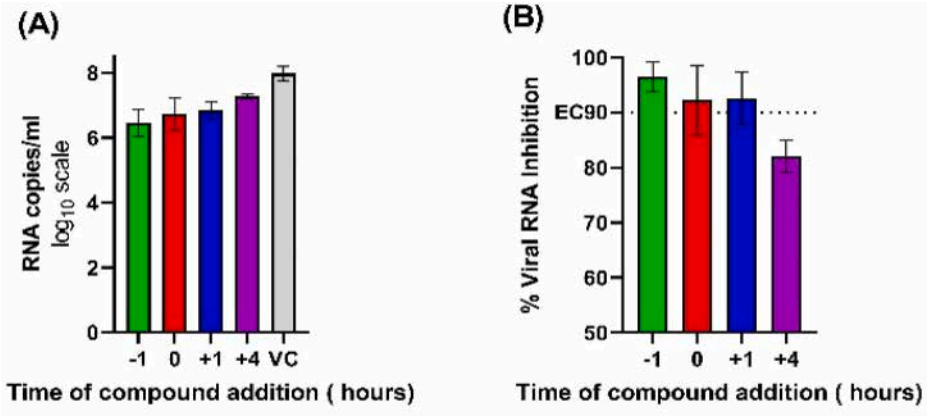

Fig. 3. Time of addition experiment of HR-568 at 10 μM in RD cells A) measured in viral RNA copies/ml and B) % viral RNA inhibition.

Table 6
In vitro anti-EV-A71 activity and cytotoxicity of promising candidates on CHO, MRC-5, and RD cells.[a]

Compound	EC_{50} (MRC-5, EV-A71)[b]	CC_{50} (MRC-5)[c]	SI (MRC-5)[d]	EC_{50} (RD, EV-A71)[b]	CC_{50} (RD)[c]	SI (RD)[d]	CC_{50} (CHO)[b]
HR-394 = 6	>40	/	/	4.65	96.29	20.7	33.56 ± 2.56
HR-267 = 9a	<0.37	>20	>54	24.68	44.66	1.81	36.89 ± 1.98
OM1260 = 5j	0.71	>20	>28	4.61	30.54	6.62	31.26 ± 2.06
HR-568 = 5f	3.16	>40	>13	1.53	23.51	15.4	43.18 ± 2.96

[a] Values reported as median ± std are from two independent experiments.
[b] EC_{50} = 50 % effective concentration (concentration at which 50 % inhibition of virus-induced cell death is observed).
[c] CC_{50} = 50 % cytotoxic concentration (concentration at which 50 % adverse effect is observed on host cell viability).
[d] SI = selectivity index for EV-A71, SI=CC_{50}/EC_{50}.

2.5. In silico pharmacokinetic evaluation of broad-spectrum inhibitors

Our compounds contain numerous aromatic cycles and interact with a hydrophobic pocket. Thus, solubility and bioavailability should be impacted by physicochemical properties related to the data. The analysis of pharmacokinetic parameters seems essential in the preclinical evaluation phases. To evaluate these parameters, we used GastroPlus™ (Version 9.9; Simulations Plus, Inc., Lancaster, California, USA) to predict pharmacokinetic parameters [Table 7].

Solubility in water, according to pH, influences the solubilization of compounds in the intestinal tract for absorption, and in blood for distribution. Log P and permeability measure the capacity to pass through cell membranes. Molar mass is involved in this process with an inversely proportional correlation [25]. Fraction absorbed represents the predicted percentage of compound absorbed just after the intestinal tract absorption, while bioavailability is the percentage after hepatic metabolism.

3. Discussion

Modulating both sides, we synthesized two promising compounds, namely **OM1260** and **HR-568**, with a broad-spectrum against Enteroviruses. They have a (sub)micromolar potency against EV-A71, E30, and CVA24. To assess the druggability of these compounds, we used innovative and rigorous methods to evaluate broad-spectrum activity against EV-A71, E30, and CVA24 in 2 cell lines. In addition, to obtain a comprehensive assessment of the compounds, we also carried out an *in-silico* study of their pharmacokinetic parameters.

3.1. Assays on 2 cell lines

As described in the results section, we worked with two different cell lines.

We successfully identified compounds with micromolar activity in both cell lines (AB113, OM1260 and HR-568), which reduces the risk of cell-specific antiviral effects. Interestingly, we observe that they are more potent on MRC-5 cells than on RD cells. These differences in potency have already been observed with direct-acting antivirals such as remdesivir and sofosbuvir, where antiviral activity may depend on the cell line tested [26,27]. This could be explained either by differences in drug metabolism or stability within the cell or by the presence of the ABC transporter p-gp, which can cause the compounds to be effluxed from the cell [28,29].

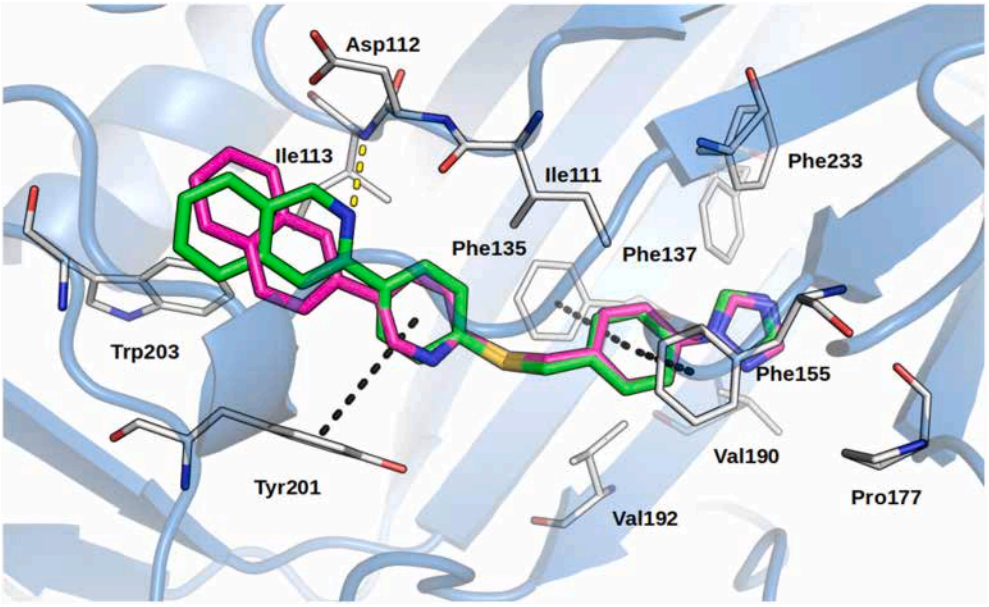

Fig. 4. Proposed binding mode for derivatives OM1260 (in green) and HR-5-068 (in magenta). Residues involved in main interactions are depicted as white stick.

Table 7
Physicochemical and absorption parameters of our most promising compounds, predicted with GatroPlus™.

Pharmacokinetic parameters	OM1260	HR-568	Vapendavir
Solubility (mg/L)	0.698	0.794	10.2
Permeability (10^{-3} cm/s)	39.9	30.8	67.6
Log P	5.28	5.19	4.00
Molecular Weight (g/mol)	394.50	394.50	382.47
Fraction absorbed (%)	83	76	100
Bioavailability (%)	81	74	92

3.2. Broad-spectrum

Even if **AB113** is more effective against EV-A71 than **OM1260** and **HR-568**, both inhibit E30 and CV-A24. These viruses belong to different species of enterovirus, respectively EV-A, EV-B, and EV-C.

We can consider that they have a broad spectrum as the capsid's hydrophobic pocket is like other viruses. Although the capsids is often the region with the highest frequency of mutation, it also has a high sequence identity among the various enterovirus species (between 55.4 % and 83.3 % in EV-A, and between 68.5 % and 87.0 % in EV-B) [30,31]. Moreover, the residues that lined the targeted hydrophobic pocket by capsid binder analyzed in RV species and on the complete Enterovirus genus [32,33]. Of the 26 amino acids in the EV-A71 hydrophobic pocket, 22 are conserved for all viruses belonging to the enterovirus genus.

3.3. Target validation

One of our working hypotheses is that our compounds target the hydrophobic canyon pocket of the capsid. This is supported by the co-crystallization of the first hit compound LPCRW_0005 in the capsid [9]. In fact, the crystal structure of HRV14 in complex with LPCRW_0005 was solved to 3.0 Å resolution to fully characterize the interactions between the compound and the viral capsid (PDB ID: 4PDW). In addition, the various modulations presented here have been modeled with a consistent binding mode. The key interactions of the molecules with the capsid have been highlighted for each hit Fig. 3.

The time-of-addition drug assay results showed a time-dependent decrease in the efficacy of our compounds when added after infection. These results confirm the inhibition of virus entry into the cell, where only the capsid is mobilized. This observation is consistent with the previously reported EV-A71 kinetic replication on rhabomyosarcoma cell line [34]. Indeed, VP1 protein is no longer detected in the cell 6 h after infection. On the contrary, from 3 h post-infection, the amount of viral RNA increases exponentially. This timing of VP1 disappearance and RNA synthesis is consistent with an activity of HR-568 on viral entry. Indeed, a decrease in activity (below 90 % of inhibition) is observed when the compound is added 4 h after infection.

The fact that this activity is not zero may be explained by a possible action at the end of the replication cycle, bearing in mind that non-lytic pathways of exit from the cell may be used by recognition of the EV-A71 capsid [35].

A large body of evidence therefore supports the link between the hydrophobic capsid pocket and our compounds as an inhibitors of enteroviruses.

3.4. Pharmacokinetic parameters

All our active compounds have similar molecular weights (less than 400 g/mol). They have a bioavailability superior to 70 %, which should mean compatibility for their development as drugs. Of note, first-pass effects appear limited for all compounds. However, the permeability of membranes to our compounds is lower than that of vapendavir. Consequently, variation in membrane permeability to our compounds does not seem to affect their bioavailability as much as might be expected.

Our broad-spectrum inhibitors (**OM1260** and **HR-568**) have a lower bioavailability than vapendavir. This could be explained by a one-grade higher log P and a predicted solubility 100 times lower.

4. Materials and methods

4.1. Chemistry

4.1.1. General methods

Commercially available reagents and solvents were used without further purification. Reactions were monitored by thin-layer chromatography (plates coated with silica gel 25 DC-Fertigfolien from Macherey-Nagel).

^{1}H and ^{13}C NMR spectra were recorded at room temperature in deuterated solvents on a Brüker Avance-250 instrument (250 MHz), a

Brüker Avance III nanobay-300 MHz or a Brüker Avance III nanobay-400 MHz. Chemical shifts (δ) are reported in parts per million (ppm) relative to the solvent [^{1}H: (δ (DMSO) = 2.50 ppm, (δ(CDCl3) = 7.26 ppm; ^{13}C: (δ (DMSO) = 39.52 ppm, (δ (CDCl3) = 77.16 ppm]. Data are reported as follows: chemical shift, type of carbon (for ^{13}C NMR), multiplicity, coupling constant in Hertz, integration, and position on the molecule. Two-dimensional spectroscopy (HSQC and HMBC) was used to assist in assignment (data not shown).

Accurate mass measurements (HRMS) were recorded on a TOF spectrometer, by the Spectropole of Faculté des Sciences de Saint Jérôme, Marseille (France). The purity of tested compounds was determined as > 95 % by liquid chromatography (LC).

In accordance with our reported works, each synthesized compound was obtained using previous synthesis pathways [7].

Likewise, compounds **1d**, **1f**, **2d**, **2f**, **3d**, **3f**, **4d**, **4f**, **4h**, and **7** were already described in previous reported works [7].

4.1.2. Products of Suzuki Miyaura cross-coupling

*4.1.2.1. 4-(1-methyl-1H-pyrazol-4-yl)benzaldehyde (**1a**).* ^{1}H NMR (400 MHz, Chloroform-*d*) δ 9.96 (s, 1H, H^{CHO}), 7.86 (dt J = 8.4, 1.9 Hz, 2H, H^{Ph}), 7.84 (s, 1H, H^{Prz}), 7.72 (s, 1H, H^{Prz}), 7.61 (dt, J = 8.4, 1.9 Hz, 2H, H^{Ph}), 3.96 (s, 3H, H^{NMe}).

^{13}C NMR (101 MHz, Chloroform-*d*) δ 191.72 (CH, 1C, C^{CHO}), 139.01 (C_q, 1C, C^{Ph}), 137.34 (CH, 1C, C^{Prz}), 134.49 (C_q, 1C, C^{Ph}), 130.69 (CH, 2C, C^{Ph}), 127.94 (CH, 1C, C^{Prz}), 125.67 (CH, 2C, C^{Ph}), 122.14 (C_q, 1C, C^{Prz}), 39.37 (CH, 1C, C^{NMe}).

*4.1.2.2. 4-(1-benzyl-1H-pyrazol-4-yl)benzaldehyde (**1b**).* ^{1}H NMR (400 MHz, Chloroform-*d*) δ 9.97 (s, 1H, H^{CHO}), 7.91 (d, J = 0.9 Hz, 1H, H^{Prz}), 7.85 (dt, J = 8.4, 1.9 Hz, 2H, H^{Ph}), 7.72 (d, J = 0.9 Hz, 1H, H^{Prz}), 7.61 (dt, J = 8.0, 1.7 Hz, 2H, H^{Ph}), 7.37 (dt + m, J = 8.0, 1.7 Hz, 3H, H^{Bz}), 7.28 (dd, J = 7.5, 1.5 Hz, 2H, H^{Bz}), 5.36 (s, 2H, H^{Bz}).

^{13}C NMR (101 MHz, Chloroform-*d*) δ 191.73 (CH, 1C, C^{CHO}), 138.94 (C_q, 1C, C^{Ph}), 137.59 (CH, 1C, C^{Prz}), 136.06 (C_q, 1C, C^{Bz}), 134.58 (C_q, 1C, C^{Ph}), 130.68 (CH, 2C, C^{Ph}), 129.14 (CH, 2C, C^{Bz}), 128.54 (CH, 1C, C^{Bz}), 128.02 (CH, 2C, C^{Bz}), 127.17 (CH, 1C, C^{Prz}), 125.74 (CH, 2C, C^{Ph}), 122.47 (C_q, 1C, C^{Prz}), 56.61 (CH_2, 1C, C^{Bz}).

*4.1.2.3. 4-(3,5-dimethylisoxazol-4-yl)benzaldehyde (**1c**).* ^{1}H NMR (400 MHz, Chloroform-*d*) δ 10.05 (s, 1H, H^{CHO}), 7.96 (dt, J = 8.3, 1.8 Hz, 2H, H^{Ph}), 7.44 (dt, J = 8.3, 1.8 Hz, 2H, H^{Ph}), 2.45 (s, 3H, H^{Me}), 2.31 (s, 3H, H^{Me}).

^{13}C NMR (101 MHz, Chloroform-*d*) δ 191.72 (CH, 1C, C^{CHO}), 166.17 (C_q, 1C, C^{Isx}), 158.43 (C_q, 1C, C^{Isx}), 137.07 (C_q, 1C, C^{Ph}), 135.45 (C_q, 1C, C^{Ph}), 130.30 (CH, 2C, C^{Ph}), 129.65 (CH, 2C, C^{Ph}), 116.00 (C_q, 1C, C^{Isx}), 11.90 (CH_3, 1C, C^{Me}), 11.03 (CH_3, 1C, C^{Me}).

*4.1.2.4. 3'-(dimethylamino)-[1,1'-biphenyl]-4-carbaldehyde (**1e**).* ^{1}H NMR (400 MHz, Chloroform-*d*) δ 10.06 (s, 1H, H^{CHO}), 7.94 (dt, J = 8.2, 1.9 Hz, 2H, H^{Ph}), 7.76 (dt, J = 8.2, 1.9 Hz, 2H, H^{Ph}), 7.35 (dd, J = 8.3, 7.6 Hz, 1H, H^{Ph}), 6.98 (dt, J = 7.6, 1.0 Hz, 1H, H^{Ph}), 6.94 (t, J = 2.6 Hz, 1H, H^{Ph}), 6.80 (ddd, J = 8.3, 2.6, 1.0 Hz, 1H, H^{Ph}), 3.03 (s, 6H, H^{NMe}).

^{13}C NMR (101 MHz, Chloroform-*d*) δ 192.16 (CH, 1C, C^{CHO}), 151.14 (C_q, 1C, C^{Ph}), 148.50 (C_q, 1C, C^{Ph}), 140.89 (C_q, 1C, C^{Ph}), 135.24 (C_q, 1C, C^{Ph}), 130.30 (CH, 2C, C^{Ph}), 129.82 (CH, 2C, C^{Ph}), 128.00 (CH, 1C, C^{Ph}), 115.92 (CH, 1C, C^{Ph}), 112.77 (CH, 1C, C^{Ph}), 111.49 (CH, 1C, C^{Ph}), 40.77 (CH, 2C, C^{NMe}).

*4.1.2.5. 2-((4-(1-methyl-1H-pyrazol-4-yl)benzyl)thio)-5-(naphthalen-2-yl)pyridine (**5a**).* ^{1}H NMR (400 MHz, Chloroform-*d*) δ 8.84 (dd, J = 2.5, 0.9 Hz, 1H, H^{Py}), 8.01 (d, J = 1.9 Hz, 1H, H^{Nph}), 7.94 (d, J = 8.5 Hz, 1H, H^{Nph}), 7.89 (dd, J = 6.9, 2.5 Hz, 1H, H^{Nph}), 7.87 (dd, J = 6.9, 2.5 Hz, 1H, H^{Nph}), 7.82 (dd, J = 8.4, 2.5 Hz, 1H, H^{Py}), 7.74 (d, J = 0.9 Hz, 1H, H^{Prz}), 7.69 (dd, J = 8.5, 1.9 Hz, 1H, H^{Nph}), 7.58 (d, J = 0.9 Hz, 1H, H^{Prz}), 7.52 (m, 2H, H^{Nph}), 7.43 (dt, J = 8.5, 1.5 Hz, 2H, H^{Ph}), 7.41 (dt, J = 8.5, 1.5 Hz, 2H, H^{Ph}), 7.28 (dd, J = 8.4, 0.9 Hz, 1H, H^{Prz}), 4.50 (s, 2H, H^{CS}), 3.93 (s, 3H, H^{NMe}).

^{13}C NMR (101 MHz, Chloroform-*d*) δ 157.78 (C_q, 1C, C^{Py}), 148.08 (CH, 1C, C^{Py}), 136.91 (CH, 1C, C^{Prz}), 136.21 (C_q, 1C, C^{Ph}), 135.03 (C_q, 1C, C^{Nph}), 134.89 (CH, 1C, C^{Py}), 133.79 (C_q, 1C, C^{Nph}), 132.92 (C_q, 1C, C^{Py}), 132.85 (C_q, 1C, C^{Nph}), 131.72 (C_q, 1C, C^{Ph}), 129.65 (CH, 2C, C^{Ph}), 129.02 (CH, 1C, C^{Nph}), 128.31 (CH, 1C, C^{Nph}), 127.86 (CH, 1C, C^{Nph}), 127.01 (CH, 1C, C^{Nph}), 126.75 (CH, 1C, C^{Prz}), 126.46 (CH, 1C, C^{Nph}), 125.78 (CH, 2C, C^{Ph}), 125.75 (CH, 1C, C^{Nph}), 124.96 (CH, 1C, C^{Nph}), 123.11 (C_q, 1C, C^{Prz}), 122.21 (CH, 1C, C^{Py}), 39.24 (CH, 1C, C^{NMe}), 34.51 (CH_2, 1C, C^{CS}).

HRMS (ESI): calcd for $C_{26}H_{21}N_3S$ [M + H]$^+$, 407.1456; observed, 407.1456.

*4.1.2.6. 2-((4-(1-benzyl-1H-pyrazol-4-yl)benzyl)thio)-5-(naphthalen-2-yl)pyridine (**5b**).* ^{1}H NMR (400 MHz, Chloroform-*d*) δ 8.83 (dd, J = 2.1, 0.9 Hz, 1H, H^{Py}), 8.01 (d, J = 2.0 Hz, 1H, H^{Nph}), 7.94 (d, J = 8.9 Hz, 1H, H^{Nph}), 7.90 (dd, 1H, H^{Nph}), 7.86 (dd, J = 7.4, 2.6 Hz, 1H, H^{Nph}), 7.82 (dd, J = 8.3, 2.4, 1H, H^{Nph}), 7.80 (d, J = 0.9 Hz, 1H, H^{Prz}), 7.68 (dd, J = 8.5, 2.1 Hz, 1H, H^{Py}), 7.59 (d, J = 0.9 Hz, 1H, H^{Prz}), 7.52 (m, 2H, H^{Nph}), 7.43 (dt, J = 8.6, 2.5 Hz, 2H, H^{Ph}), 7.40 (dt, J = 8.6, 2.5 Hz, 2H, H^{Ph}), 7.34 (m, 3H, H^{Bz}), 7.28 (dd, J = 8.5, 0.9 Hz, 1H, H^{Py}), 7.24 (dd, J = 7.8, 1.4 Hz, 2H, H^{Bz}), 5.33 (s, 2H, H^{Bz}), 4.49 (s, 2H, H^{CS}).

^{13}C NMR (101 MHz, Chloroform-*d*) δ 157.77 (C_q, 1C, C^{Py}), 148.07 (CH, 1C, C^{Py}), 137.15 (CH, 1C, C^{Prz}), 136.52 (C_q, 1C, C^{Ph}), 136.27 (C_q, 1C, C^{Bz}), 135.02 (C_q, 1C, C^{Nph}), 134.88 (CH, 1C, C^{Py}), 133.79 (C_q, 1C, C^{Nph}), 132.92 (C_q, 1C, C^{Py}), 132.85(C_q, 1C, C^{Nph}), 131.60 (C_q, 1C, C^{Ph}), 129.65 (CH, 2C, C^{Ph}), 129.03 (CH, 2C, C^{Bz}), 129.02 (CH, 1C, C^{Nph}), 128.31 (CH, 1C, C^{Bz}), 127.88 (CH, 2C, C^{Bz}), 127.87 (CH, 1C, C^{Nph}), 126.75 (CH, 1C, C^{Nph}), 126.46 (CH, 2C, C^{Nph}), 126.29 (CH, 1C, C^{Prz}), 125.76 (CH, 2C, C^{Ph}), 125.75 (CH, 1C, C^{Nph}), 124.96 (CH, 1C, C^{Nph}), 123.38 (C_q, 1C, C^{Prz}), 122.22 (CH, 1C, C^{Py}), 56.40 (CH_2, 1C, C^{Bz}), 34.53 (CH_2, 1C, C^{CS}).

HRMS (ESI): calcd for $C_{32}H_{25}N_3S$ [M + H]$^+$, 483.1769; observed, 483.1769.

*4.1.2.7. 3,5-dimethyl-4-(4-(((5-(naphthalen-2-yl)pyridin-2-yl)thio)methyl)phenyl)isoxazole (**5c**).* ^{1}H NMR (400 MHz, Chloroform-*d*) δ 8.85 (dd, J = 2.5, 0.9 Hz, 1H, H^{Py}), 8.02 (d, J = 2.0 Hz, 1H, H^{Nph}), 7.95 (d, J = 8.7 Hz, 1H, H^{Nph}), 7.91 (dd, J = 7.3, 2.7 Hz, 1H, H^{Nph}), 7.88 (dd, J = 7.3, 2.7 Hz, 1H, H^{Nph}), 7.85 (dd, J = 8.4, 2.5 Hz, 1H, H^{Py}), 7.70 (dd, J = 8.7, 2.0 Hz, 1H, H^{Nph}), 7.52 (dt + m, J = 8.5, 2.0 Hz, 4H, $H^{Ph + Naph}$), 7.31 (dd, J = 8.4, 0.9 Hz, 1H, H^{Py}), 7.21 (dt, J = 8.5, 2.0 Hz, 2H, H^{Ph}), 4.55 (s, 2H, H^{CS}), 2.40 (s, 3H, H^{Me}), 2.27 (s, 3H, H^{Me}).

^{13}C NMR (101 MHz, Chloroform-*d*) δ 165.37 (C_q, 1C, C^{Isx}), 158.87 (C_q, 1C, C^{Isx}), 157.47 (C_q, 1C, C^{Py}), 148.10 (CH, 1C, C^{Py}), 137.75 (C_q, 1C, C^{Ph}), 134.95 (CH, 1C, C^{Py}), 133.79 (C_q, 1C, C^{Nph}), 132.97 (C_q, 2C, C^{Nph}), 132.94 (C_q, 1C, C^{Py}), 129.57 (CH, 2C, C^{Ph}), 129.43 (C_q, 1C, C^{Ph}), 129.33 (CH, 2C, C^{Ph}), 129.07 (CH, 1C, C^{Nph}), 128.30 (CH, 1C, C^{Nph}), 127.87 (CH, 1C, C^{Nph}), 126.79 (CH, 1C, C^{Nph}), 126.51 (CH, 1C, C^{Nph}), 125.76 (CH, 1C, C^{Nph}), 124.91 (CH, 1C, C^{Nph}), 122.19 (CH, 1C, C^{Py}), 116.47 (C_q, 1C, C^{Isx}), 34.22 (CH_2, 1C, C^{CS}), 11.75 (CH_3, 1C, C^{Me}), 11.00 (CH_3, 1C, C^{Me}).

HRMS (ESI): calcd for $C_{27}H_{22}N_3OS$ [M + H]$^+$, 422.1453; observed, 422.1453.

*4.1.2.8. N,N-dimethyl-4'-(((5-(naphthalen-2-yl)pyridin-2-yl)thio)methyl)-[1,1'-biphenyl]-4-amine (**5d**).* ^{1}H NMR (400 MHz, Chloroform-*d*) δ 8.85 (dd, J = 2.5, 0.9 Hz, 1H, H^{Py}), 8.02 (d, J = 1.9 Hz, 1H, H^{Nph}), 7.94 (d, J = 8.5 Hz, 1H, H^{Nph}), 7.90 (dd, J = 7.5, 1.8 Hz, 1H, H^{Nph}), 7.87 (dd, J = 7.5, 1.8 Hz, 1H, H^{Nph}), 7.83 (dd, J = 8.4, 2.5 Hz, 1H, H^{Py}), 7.70 (dd, J = 8.5, 1.9 Hz, 1H, H^{Nph}), 7.52 (m, 5H, $H^{Nph + Ph}$), 7.47 (m, 3H, $H^{Nph + Ph}$), 7.29 (dd, J = 8.4, 0.9 Hz, 1H, H^{Py}), 6.80 (dt, J = 8.8, 2.6 Hz, 2H, H^{Ph}), 4.53 (s, 2H, H^{CS}), 2.99 (s, 6H, H^{NMe}).

^{13}C NMR (101 MHz, Chloroform-*d*) δ 157.99 (C_q, 1C, C^{Py}), 150.11 (C_q, 1C, C^{Ph}), 148.09 (CH, 1C, C^{Py}), 140.29 (C_q, 1C, C^{Ph}), 135.69 (C_q, 1C, C^{Ph}), 135.08 (C_q, 1C, C^{Nph}), 134.88 (CH, 1C, C^{Py}), 133.80 (C_q, 1C, C^{Ph}), 132.91 (C_q, 1C, C^{Py}), 132.80 (C_q, 1C, C^{Nph}), 129.47 (CH, 2C, C^{Ph}), 129.01 (CH, 1C, C^{Nph}), 128.32 (CH, 1C, C^{Nph}), 127.86 (CH, 1C, C^{Nph}), 127.76 (CH, 2C, C^{Ph}), 126.73 (CH, 1C, C^{Nph}), 126.53 (CH, 2C, C^{Ph}), 126.43 (CH, 1C, C^{Nph}), 125.75(CH, 1C, C^{Nph}), 124.99(CH, 1C, C^{Nph}), 122.17 (CH, 1C, C^{Py}), 112.91 (CH, 2C, C^{Ph}), 111.65 (C_q, 1C, C^{Nph}), 40.72 (CH, 2C, C^{NMe}), 34.56 (CH, 1C, C^{CS}).

HRMS (ESI): calcd for $C_{30}H_{26}N_2S$ $[M + H]^+$, 446.1817; observed, 446.1817.

*4.1.2.9. N,N-dimethyl-4'-(((5-(naphthalen-2-yl)pyridin-2-yl)thio) methyl)-[1,1′-biphenyl]-3-amine (**5e**).* ^{1}H NMR (400 MHz, Chloroform-*d*) δ 8.86 (dd, $J = 2.5$, 0.9 Hz, 1H, H^{Py}), 8.02 (d, $J = 1.9$ Hz, 1H, H^{Nph}), 7.95 (d, $J = 8.5$ Hz, 1H, H^{Nph}), 7.91 (dd, $J = 7.3$, 2.3 Hz, 1H, H^{Nph}), 7.88 (dd, $J = 7.3$, 2.3 Hz, 1H, H^{Nph}), 7.83 (dd, $J = 8.3$, 2.5 Hz, 1H, H^{Py}), 7.70 (dd, $J = 8.5$, 1.9 Hz, 2H, H^{Ph}), 7.56 (dt, $J = 8.5$, 1.9 Hz, 2H, H^{Ph}), 7.51 (d + m, $J = 8.5$ Hz, 3H, H^{Nph}), 7.30 (dd + dd, $J = 8.3$, 7.5, 0.9 Hz, 2H, $H^{Ph + Py}$), 6.94 (ddd, $J = 7.5$, 1.7, 0.9 Hz, 1H, H^{Ph}), 6.92 (dd, $J = 2.5$, 1.7 Hz, 1H, H^{Ph}), 6.74 (ddd, $J = 8.3$, 2.5, 0.9 Hz, 1H, H^{Ph}), 4.56 (s, 2H, H^{CS}), 3.00 (s, 6H, H^{NMe}).

^{13}C NMR (101 MHz, Chloroform-*d*) δ 157.82 (C_q, 1C, C^{Py}), 151.05 (C_q, 1C, C^{Ph}), 148.08 (CH, 1C, C^{Py}), 142.02 (C_q, 1C, C^{Ph}), 141.28 (C_q, 1C, C^{Ph}), 137.02 (C_q, 1C, C^{Ph}), 135.03 (C_q, 1C, C^{Nph}), 134.88 (CH, 1C, C^{Py}), 133.78 (C_q, 1C, C^{Nph}), 132.91 (C_q, 1C, C^{Py}), 132.82 (C_q, 1C, C^{Nph}), 129.54 (CH, 1C, C^{Ph}), 129.39 (CH, 2C, C^{Ph}), 129.01 (CH, 1C, C^{Ph}), 128.31 (CH, 1C, C^{Ph}), 127.85 (CH, 1C, C^{Ph}), 127.61 (CH, 2C, C^{Ph}), 126.73 (CH, 1C, C^{Ph}), 126.44 (CH, 1C, C^{Ph}), 125.74 (CH, 1C, C^{Ph}), 124.96 (CH, 1C, C^{Ph}), 122.17 (CH, 1C, C^{Py}), 115.91 (CH, 1C, C^{Ph}), 111.79 (CH, 1C, C^{Ph}), 111.63 (CH, 1C, C^{Ph}), 40.85 (CH, 2C, C^{NMe}), 34.45 (CH, 1C, C^{CS}).

HRMS (ESI): calcd for $C_{30}H_{26}N_2S$ $[M + H]^+$, 446.1817; observed, 446.1817.

*4.1.2.10. 2-((4-(1H-1,2,4-triazol-1-yl)benzyl)thio)-5-(naphthalen-2-yl) pyridine (**5f**).* ^{1}H NMR (400 MHz, DMSO-d_6) δ 9.26 (s, 1H, H^{Trz}), 8.97 (dd, $J = 2.5$, 1.0 Hz, 1H, H^{Py}), 8.30 (d, $J = 2.0$ Hz, 1H, H^{Nph}), 8.22 (s, 1H, H^{Trz}), 8.13 (dd, $J = 8.4$, 2.5 Hz, 1H, H^{Py}), 8.04 (d, $J = 8.7$ Hz, 1H, H^{Nph}), 8.00 (dd, $J = 6.3$, 2.6 Hz, 1H, H^{Nph}), 7.96 (dd, $J = 6.3$, 2.6 Hz, 1H, H^{Nph}), 7.89 (dd, $J = 8.7$, 2.0 Hz, 1H, H^{Nph}), 7.81 (dt, $J = 8.7$, 2.3 Hz, 2H, H^{Ph}), 7.65 (dt, $J = 8.7$, 2.3 Hz, 2H, H^{Ph}), 7.56 (m, 2H, H^{Nph}), 7.48 (dd, $J = 8.4$, 1.0 Hz, 1H, H^{Py}), 4.57 (s, 2H, H^{CS}).

^{13}C NMR (101 MHz, DMSO-d_6) δ 157.26 (C_q, 1C, C^{Py}), 152.86 (CH, 1C, C^{Trz}), 148.00 (CH, 1C, C^{Py}), 142.75 (CH, 1C, C^{Trz}), 138.49 (C_q, 1C, C^{Ph}), 136.12 (C_q, 1C, C^{Ph}), 135.47 (CH, 1C, C^{Py}), 134.37 (C_q, 1C, C^{Nph}), 133.77 (C_q, 1C, C^{Nph}), 132.88 (C_q, 1C, C^{Nph}), 132.26 (C_q, 1C, C^{Py}), 130.67 (CH, 2C, C^{Ph}), 129.20 (CH, 1C, C^{Nph}), 128.67 (CH, 1C, C^{Nph}), 128.04 (CH, 1C, C^{Nph}), 127.07 (CH, 1C, C^{Nph}), 126.89 (CH, 1C, C^{Nph}), 125.72 (CH, 1C, C^{Nph}), 125.06 (CH, 1C, C^{Nph}), 122.30 (CH, 1C, C^{Py}), 119.97 (CH, 2C, C^{Ph}), 33.18 (CH_2, 1C, C^{CS}).

HRMS (ESI): calcd for $C_{23}H_{17}N_5S$ $[M + H]^+$, 394.1252; observed, 394.1252.

*4.1.2.11. 3-(6-((4-(1H-1,2,4-triazol-1-yl)benzyl)thio)pyridin-3-yl)iso-quinoline (**5g**).* ^{1}H NMR (400 MHz, DMSO-d_6) δ 9.29 (d, $J = 2.4$ Hz, 1H, H^{Qnl}), 9.25 (s, 1H, H^{Trz}), 9.03 (dd, $J = 2.5$, 1.0 Hz, 1H, H^{Py}), 8.73 (d, $J = 2.4$ Hz, 1H, H^{Qnl}), 8.22 (s, 1H, H^{Trz}), 8.20 (dd, $J = 8.4$, 2.5 Hz, 1H, H^{Py}), 8.07 (dd, $J = 8.4$, 1.5 Hz, 1H, H^{Qnl}), 8.04 (dd, $J = 8.4$, 1.5 Hz, 1H, H^{Qnl}), 7.81 (dt, $J = 8.6$, 2.1 Hz, 2H, H^{Ph}), 7.78 (dd, $J = 6.9$, 1.5 Hz, 1H, H^{Qnl}), 7.67 (dd, $J = 6.9$, 1.5 Hz, 1H, H^{Qnl}), 7.64 (dt, $J = 8.6$, 2.1 Hz, 2H, H^{Ph}), 7.52 (dd, $J = 8.4$, 1.0 Hz, 1H, H^{Py}), 4.57 (s, 2H, H^{CS}).

^{13}C NMR (101 MHz, DMSO-d_6) δ 158.10 (C_q, 1C, C^{Py}), 152.85 (CH, 1C, C^{Trz}), 149.51 (CH, 1C, C^{Qnl}), 148.15 (CH, 1C, C^{Py}), 147.42 (C_q, 1C, C^{Qnl}), 142.75 (CH, 1C, C^{Trz}), 138.41 (C_q, 1C, C^{Ph}), 136.12 (C_q, 1C, C^{Ph}), 135.62 (CH, 1C, C^{Py}), 133.36 (CH, 1C, C^{Qnl}), 130.66 (CH, 2C, C^{Ph}), 130.30 (CH, 1C, C^{Qnl}), 129.98 (C_q, 1C, C^{Py}), 129.55 (C_q, 1C, C^{Qnl}), 129.19 (CH, 1C, C^{Qnl}), 128.87 (CH, 1C, C^{Qnl}), 128.04 (C_q, 1C, C^{Qnl}), 127.67 (CH, 1C, C^{Qnl}), 122.36 (CH, 1C, C^{Py}), 119.96 (CH, 2C, C^{Ph}), 33.15 (CH_2, 1C, C^{CS}).

HRMS (ESI): calcd for $C_{24}H_{18}N_4S$ $[M + H]^+$, 395.1205; observed, 395.1205.

*4.1.2.12. 1-(4-(((4-(naphthalen-2-yl)phenyl)thio)methyl)phenyl)-1H-1,2,4-triazole (**5h**).* ^{1}H NMR (400 MHz, DMSO-d_6) δ 9.26 (s, 1H, H^{Trz}), 8.22 (s, 1H, H^{Trz}), 8.21 (d, $J = 1.9$ Hz, 1H, H^{Nph}), 8.00 (d, $J = 8.8$ Hz, 1H, H^{Nph}), 7.98 (dd, $J = 7.4$, 2.4 Hz, 2H, H^{Nph}), 7.94 (dd, $J = 7.5$, 2.2 Hz, 1H, H^{Nph}), 7.84 (dd, $J = 8.8$, 1.9 Hz, 1H, H^{Nph}), 7.81 (dt, $J = 8.6$, 2.3 Hz, 2H, H^{Ph}), 7.78 (dt, $J = 8.5$, 2.2 Hz, 2H, H^{Ph}), 7.59 (dt, $J = 8.6$, 2.3 Hz, 2H, H^{Ph}), 7.53 (m, 2H, H^{Nph}), 7.50 (dt, $J = 8.5$, 2.2 Hz, 2H, H^{Ph}), 4.39 (s, 2H, H^{CS}).

^{13}C NMR (101 MHz, DMSO-d_6) δ 152.87 (CH, 1C, C^{Trz}), 142.75 (CH, 1C, C^{Trz}), 138.00 (C_q, 1C, C^{Nph}), 137.93 (C_q, 1C, C^{Ph}), 137.10 (C_q, 1C, C^{Ph}), 136.14 (C_q, 1C, C^{Ph}), 135.70 (C_q, 1C, C^{Ph}), 133.82 (C_q, 1C, C^{Nph}), 132.72 (C_q, 1C, C^{Nph}), 130.62 (CH, 2C, C^{Ph}), 129.46 (CH, 2C, C^{Ph}), 128.99 (CH, 1C, C^{Nph}), 128.67 (CH, 1C, C^{Nph}), 127.97 (CH, 1C, C^{Nph}), 127.90 (CH, 2C, C^{Ph}), 126.93 (CH, 1C, C^{Nph}), 126.64 (CH, 1C, C^{Nph}), 125.43 (CH, 1C, C^{Nph}), 125.28 (CH, 1C, C^{Nph}), 119.92 (CH, 2C, C^{Ph}), 36.34 (CH_2, 1C, C^{CS}).

HRMS (ESI): calcd for $C_{25}H_{19}N_3S$ $[M + H]^+$, 393.1300; observed, 393.1300.

*4.1.2.13. 2-((4-(1H-1,2,4-triazol-1-yl)benzyl)thio)-5-(naphthalen-1-yl) pyridine (**5i**).* ^{1}H NMR (400 MHz, DMSO-d_6) δ 9.27 (s, 1H, H^{Trz}), 8.23 (s, 1H, H^{Trz}), 8.00 (dd, $J = 8.1$, 1.5 Hz, 1H, H^{Nph}), 7.95 (dd, $J = 8.1$, 1.5 Hz, 1H, H^{Nph}), 7.82 (dt, $J = 8.5$, 2.2 Hz, 2H, H^{Ph}), 7.77 (dd, $J = 8.3$, 1.2 Hz, 1H, H^{Nph}), 7.60 (dt, $J = 8.3$, 2.1 Hz, 2H, H^{Ph}), 7.57 (dd, $J = 8.3$, 1.2 Hz, 1H, H^{Nph}), 7.54 (dd, $J = 8.0$, 1.5 Hz, 1H, H^{Nph}), 7.51 (dt, $J = 8.3$, 2.1 Hz, 2H, H^{Ph}), 7.48 (dd, $J = 8.0$, 1.5 Hz, 1H, H^{Nph}), 7.41 (dt, $J = 8.5$, 2.2 Hz, 3H, $H^{Ph + Nph}$), 4.40 (s, 2H, H^{CS}).

^{13}C NMR (101 MHz, DMSO-d_6) δ 152.88 (CH, 1C, C^{Trz}), 142.79 (CH, 1C, C^{Trz}), 139.24 (C_q, 1C, C^{Nph}), 138.10 (C_q, 1C, C^{Ph}), 137.86 (C_q, 1C, C^{Ph}), 136.17 (C_q, 1C, C^{Ph}), 135.64 (C_q, 1C, C^{Ph}), 133.94 (C_q, 1C, C^{Nph}), 131.22 (C_q, 1C, C^{Nph}), 130.83 (CH, 2C, C^{Ph}), 130.67 (CH, 2C, C^{Ph}), 128.88 (CH, 3C, $C^{Nph + Ph}$), 128.22 (CH, 1C, C^{Nph}), 127.34 (CH, 1C, C^{Nph}), 126.93 (CH, 1C, C^{Nph}), 126.47 (CH, 1C, C^{Nph}), 126.09 (CH, 1C, C^{Nph}), 125.57 (CH, 1C, C^{Nph}), 119.91 (CH, 2C, C^{Ph}), 36.42 (CH_2, 1C, C^{CS}).

HRMS (ESI): calcd for $C_{25}H_{19}N_3S$ $[M + H]^+$, 393.1300; observed, 393.1300.

*4.1.2.14. 3-(4-((4-(1H-1,2,4-triazol-1-yl)benzyl)thio)phenyl)isoquinoline (**5j**).* ^{1}H NMR (400 MHz, DMSO-d_6) δ 9.26 (s, 1H, H^{Trz}), 9.24 (d, $J = 2.4$ Hz, 1H, H^{Qnl}), 8.64 (dd, $J = 2.4$ Hz, 2H, H^{Qnl}), 8.22 (s, 1H, H^{Trz}), 8.05 (t, $J = 8.5$, 1.2 Hz, 1H, H^{Qnl}), 8.03 (t, $J = 8.5$, 1.2 Hz, 1H, H^{Qnl}), 7.84 (dt, $J = 8.6$, 2.2 Hz, 2H, H^{Ph}), 7.81 (dt, $J = 8.7$, 2.3 Hz, 2H, H^{Ph}), 7.76 (ddd, $J = 8.3$, 6.9, 1.5 Hz, 1H, H^{Qnl}), 7.64 (ddd, $J = 8.3$, 6.9, 1.5 Hz, 1H, H^{Qnl}), 7.60 (dt, $J = 8.7$, 2.3 Hz, 2H, H^{Ph}), 7.53 (dt, $J = 8.6$, 2.2 Hz, 2H, H^{Ph}), 4.41 (s, 2H, H^{CS}).

^{13}C NMR (101 MHz, DMSO-d_6) δ 152.86 (CH, 1C, C^{Trz}), 149.71 (CH, 1C, C^{Qnl}), 147.27 (C_q, 1C, C^{Qnl}), 142.75 (CH, 1C, C^{Trz}), 137.81 (C_q, 1C, C^{Ph}), 136.69 (C_q, 1C, C^{Ph}), 136.16 (C_q, 1C, C^{Ph}), 134.96 (C_q, 1C, C^{Ph}), 132.97 (CH, 1C, C^{Qnl}), 132.46 (C_q, 1C, C^{Qnl}), 130.61 (CH, 2C, C^{Ph}), 130.02 (CH, 1C, C^{Qnl}), 129.31 (CH, 2C, C^{Ph}), 128.15 (C_q, 1C, C^{Qnl}), 128.07 (CH, 2C, C^{Ph}), 127.54 (CH, 1C, C^{Qnl}), 119.93 (CH, 2C, C^{Ph}), 36.09 (CH_2, 1C, C^{CS}).

HRMS (ESI): calcd for $C_{24}H_{18}N_4S$ $[M + H]^+$, 394.1252; observed, 394.1252.

*4.1.2.15. 1-(4-(((4-(benzofuran-2-yl)phenyl)thio)methyl)phenyl)-1H-1,2,4-triazole (**5k**).* ^{1}H NMR (400 MHz, DMSO-d_6) δ 9.25 (s, 1H, H^{Trz}), 8.22 (s, 1H, H^{Trz}), 7.84 (dt, J = 8.5, 2.2 Hz, 2H, H^{Ph}), 7.79 (dt, J = 8.5, 2.3 Hz, 2H, H^{Ph}), 7.65 (dd, J = 7.7, 1.0 Hz, 1H, H^{Fur}), 7.61 (dd, J = 7.7, 1.0 Hz, 1H, H^{Fur}), 7.57 (dt, J = 8.5, 2.3 Hz, 2H, H^{Ph}), 7.48 (dt, J = 8.5, 2.2 Hz, 2H, H^{Ph}), 7.42 (d, J = 1.0 Hz, 1H, H^{Fur}), 7.32 (td, J = 7.5, 1.5 Hz, 1H, H^{Fur}), 7.25 (td, J = 7.5, 1.5 Hz, 1H, H^{Fur}), 4.40 (s, 2H, H^{CS}).

^{13}C NMR (101 MHz, DMSO-d_6) δ 155.23 (C_q, 1C, C^{Fur}), 154.66 (C_q, 1C, C^{Fur}), 152.87 (CH, 1C, C^{Trz}), 142.73 (CH, 1C, C^{Trz}), 137.68 (C_q, 1C, C^{Ph}), 137.35 (C_q, 1C, C^{Ph}), 136.17 (C_q, 1C, C^{Ph}), 130.66 (CH, 2C, C^{Ph}), 129.34 (C_q, 1C, C^{Fur}), 129.05 (CH, 2C, C^{Ph}), 127.73 (C_q, 1C, C^{Ph}), 125.62 (CH, 2C, C^{Ph}), 125.10 (CH, 1C, C^{Fur}), 123.78 (CH, 1C, C^{Fur}), 121.61 (CH, 1C, C^{Fur}), 119.92 (CH, 2C, C^{Ph}), 111.56 (CH, 1C, C^{Fur}), 102.40 (CH, 1C, C^{Fur}), 36.03 (CH_2, 1C, C^{CS}).

HRMS (ESI): calcd for $C_{23}H_{17}N_3OS$ $[M + H]^+$, 383.1092; observed, 383.1092.

*4.1.2.16. 5-(4-((4-(1H-1,2,4-triazol-1-yl)benzyl)thio)phenyl)-1H-indole (**5l**).* ^{1}H NMR (400 MHz, DMSO-d_6) δ 11.15 (s, 1H, H^{NH}), 9.25 (s, 1H, H^{Trz}), 8.21 (s, 1H, H^{Trz}), 7.80 (dt, J = 8.6, 2.3 Hz, 2H, H^{Ph}), 7.61 (dt, J = 8.4, 2.3 Hz, 3H, $H^{Ind + Ph}$), 7.58 (s, 1H, H^{Ind}), 7.56 (dt, J = 8.6, 2.4 Hz, 2H, H^{Ph}), 7.43 (dt, J = 8.4, 2.3 Hz, 2H, H^{Ph}), 7.37 (t, J = 2.8 Hz, 1H, H^{Ind}), 7.28 (dd, J = 8.3, 1.8 Hz, 1H, H^{Ind}), 6.43 (t, J = 2.8 Hz, 1H, H^{Ind}), 4.35 (s, 2H, H^{CS}).

^{13}C NMR (101 MHz, DMSO-d_6) δ 152.87 (CH, 1C, C^{Trz}), 142.74 (CH, 1C, C^{Trz}), 139.99 (C_q, 1C, C^{Ph}), 138.07 (C_q, 1C, C^{Ph}), 136.98 (C_q, 1C, C^{Ind}), 136.12 (C_q, 1C, C^{Ph}), 134.06 (C_q, 1C, C^{Ph}), 132.95 (C_q, 1C, C^{Ind}), 130.61 (CH, 2C, C^{Ph}), 129.79 (CH, 2C, C^{Ph}), 127.70 (C_q, 1C, C^{Ind}), 127.64 (CH, 2C, C^{Ph}), 126.78 (CH, 1C, C^{Ind}), 120.95 (CH, 1C, C^{Ind}), 119.89 (CH, 2C, C^{Ph}), 118.51 (CH, 1C, C^{Ind}), 109.64 (CH, 1C, C^{Ind}), 101.45 (CH, 1C, C^{Ind}), 36.73 (CH_2, 1C, C^{CS}).

HRMS (ESI): calcd for $C_{23}H_{20}N_4S$ $[M + H]^+$, 382.1252; observed, 382.1252.

*4.1.2.17. 6-(4-((4-(1H-1,2,4-triazol-1-yl)benzyl)thio)phenyl)-1H-indazole (**5m**).* ^{1}H NMR (400 MHz, DMSO-d_6) δ 13.11 (s, 1H, H^{NH}), 9.25 (s, 1H, H^{Trz}), 8.22 (s, 1H, H^{Trz}), 8.11 (s, 1H, H^{Idz}), 8.01 (s, 1H, H^{Idz}), 7.80 (d, J = 8.5 Hz, 2H, H^{Ph}), 7.64 (d, J = 8.4 Hz, 3H, $H^{Idz + Ph}$), 7.60 (d, J = 8.6 Hz, 1H, H^{Idz}), 7.56 (d, J = 8.6 Hz, 2H, H^{Ph}), 7.44 (d, J = 8.4 Hz, 2H, H^{Ph}), 4.35 (s, 2H, H^{CS}).

^{13}C NMR (101 MHz, DMSO-d_6) δ 152.85 (CH, 1C, C^{Trz}), 142.72 (CH, 1C, C^{Trz}), 139.84 (C_q, 1C, C^{Idz}), 139.07 (C_q, 1C, C^{Ph}), 137.99 (C_q, 1C, C^{Ph}), 136.12 (C_q, 1C, C^{Ph}), 134.52 (C_q, 1C, C^{Ph}), 134.48 (CH, 1C, C^{Idz}), 132.36 (C_q, 1C, C^{Idz}), 130.60 (CH, 2C, C^{Ph}), 129.67 (CH, 2C, C^{Ph}), 127.75 (CH, 2C, C^{Ph}), 125.85 (CH, 1C, C^{Idz}), 124.02 (C_q, 1C, C^{Idz}), 119.88 (CH, 2C, C^{Ph}), 118.54 (CH, 1C, C^{Idz}), 111.06 (CH, 1C, C^{Idz}), 36.58 (CH_2, 1C, C^{CS}).

HRMS (ESI): calcd for $C_{22}H_{19}N_5S$ $[M + H]^+$, 383.1205; observed, 383.1205.

*4.1.2.18. (3-(6-((4-(1H-1,2,4-triazol-1-yl)benzyl)thio)pyridin-3-yl)phenyl)methanol (**5n**).* ^{1}H NMR (400 MHz, DMSO-d_6) δ 9.25 (s, 1H, H^{Trz}), 8.79 (dd, J = 2.5, 1.0 Hz, 1H, H^{Py}), 8.21 (s, 1H, H^{Trz}), 7.95 (dd, J = 8.4, 2.5 Hz, 1H, H^{Py}), 7.79 (dt, J = 8.8, 2.3 Hz, 2H, H^{Ph}), 7.63 (dt + m, J = 8.8, 2.3 Hz, 3H, H^{Ph}), 7.57 (dt, J = 7.6, 1.3 Hz, 1H, H^{Ph}), 7.43 (dd + t, J = 8.4, 5.6, 1.0 Hz, 2H, $H^{Ph + Py}$), 7.35 (dt, J = 7.6, 1.3 Hz, 1H, H^{Ph}), 5.25 (t, J = 5.7 Hz, 1H, H^{OH}), 4.57 (d, J = 5.7 Hz, 2H, H^{CO}), 4.54 (s, 2H, H^{CS}).

^{13}C NMR (101 MHz, DMSO-d_6) δ 157.07 (C_q, 1C, C^{Py}), 152.86 (CH, 1C, C^{Trz}), 147.67 (CH, 1C, C^{Py}), 144.00 (C_q, 1C, C^{Ph}), 141.81 (CH, 1C, C^{Trz}), 138.47 (C_q, 1C, C^{Ph}), 136.79 (C_q, 1C, C^{Ph}), 136.11 (C_q, 1C, C^{Ph}), 135.26 (CH, 1C, C^{Py}), 132.59 (C_q, 1C, C^{Py}), 130.67 (CH, 2C, C^{Ph}), 129.42 (CH, 1C, C^{Ph}), 126.54 (CH, 1C, C^{Ph}), 125.32 (CH, 1C, C^{Ph}), 124.98 (CH, 1C, C^{Ph}), 122.25 (CH, 1C, C^{Py}), 119.95 (CH, 2C, C^{Ph}), 63.26 (CH_2, 1C, C^{CO}), 33.17 (CH_2, 1C, C^{CS}).

HRMS (ESI): calcd for $C_{21}H_{18}N_4OS$ $[M + H]^+$, 374.1201; observed, 374.1201.

*4.1.2.19. 4-(6-((4-(2-aminopyrimidin-5-yl)benzyl)thio)pyridin-3-yl)benzaldehyde (**8a**).* ^{1}H NMR (400 MHz, DMSO-d_6) δ 10.06 (s, 1H, H^{CHO}), 8.91 (d, J = 2.5 Hz, 1H, H^{Py}), 8.55 (s, 2H, H^{Pym}), 8.07 (dd, J = 8.4, 2.5 Hz, 1H, H^{Py}), 8.01 (dt, J = 8.4, 2.0 Hz, 2H, H^{Ph}), 7.97 (dt, J = 8.4, 2.0 Hz, 2H, H^{Ph}), 7.56 (dt, J = 8.4, 1.9 Hz, 2H, H^{Ph}), 7.50 (dt, J = 8.4, 2.0 Hz, 2H, H^{Ph}), 7.47 (d, J = 8.4 Hz, 1H, H^{Py}), 6.76 (s, 2H, H^{NH2}), 4.52 (s, 2H, H^{CS}).

^{13}C NMR (101 MHz, DMSO-d_6) δ 193.19 (CH, 1C, C^{CHO}), 163.38 (C_q, 1C, C^{Pym}), 158.96 (C_q, 1C, C^{Py}), 156.33 (CH, 1C, C^{Pym}), 148.10 (CH, 1C, C^{Py}), 142.85 (C_q, 1C, C^{Ph}), 137.05 (C_q, 1C, C^{Ph}), 135.84 (C_q, 1C, C^{Ph}), 135.54 (CH, 1C, C^{Py}), 134.58 (C_q, 1C, C^{Pym}), 130.97 (C_q, 1C, C^{Py}), 130.72 (CH, 2C, C^{Ph}), 130.02 (CH, 2C, C^{Ph}), 127.59 (CH, 2C, C^{Ph}), 125.76 (CH, 2C, C^{Ph}), 122.19 (C_q, 1C, C^{Ph}), 122.17 (CH, 1C, C^{Py}), 33.51 (CH_2, 1C, C^{CS}).

*4.1.2.20. 4-(6-((4-(2-(dimethylamino)pyrimidin-5-yl)benzyl)thio)pyridin-3-yl)benzaldehyde (**8b**).* ^{1}H NMR (400 MHz, DMSO-d_6) δ 10.06 (s, 1H, H^{CHO}), 8.92 (dd, J = 2.4, 0.9 Hz, 1H, H^{Py}), 8.67 (s, 2H, H^{Pym}), 8.08 (dd, J = 8.4, 2.4 Hz, 1H, H^{Py}), 8.01 (dt, J = 8.5, 2.2 Hz, 2H, H^{Ph}), 7.98 (dt, J = 8.5, 2.2 Hz, 2H, H^{Ph}), 7.58 (dt, J = 8.4, 2.1 Hz, 2H, H^{Ph}), 7.51 (dt, J = 8.4, 2.1 Hz, 2H, H^{Ph}), 7.47 (dd, J = 8.4, 0.9 Hz, 1H, H^{Py}), 4.52 (s, 2H, H^{CS}), 3.16 (s, 6H, H^{NMe}).

^{13}C NMR (101 MHz, DMSO-d_6) δ 193.22 (CH, 1C, C^{CHO}), 161.65 (C_q, 1C, C^{Pym}), 158.96 (C_q, 1C, C^{Py}), 156.00 (CH, 2C, C^{Pym}), 148.12 (CH, 1C, C^{Py}), 142.86 (C_q, 1C, C^{Ph}), 137.17 (C_q, 1C, C^{Ph}), 135.85 (C_q, 1C, C^{Ph}), 135.56 (CH, 1C, C^{Py}), 134.45 (C_q, 1C, C^{Pym}), 130.98 (C_q, 1C, C^{Py}), 130.74 (CH, 2C, C^{Ph}), 130.06 (CH, 2C, C^{Ph}), 127.61 (CH, 2C, C^{Ph}), 125.83 (CH, 2C, C^{Ph}), 122.19 (CH, 1C, C^{Py}), 121.17 (C_q, 1C, C^{Ph}), 37.21 (CH_3, 2C, C^{NMe}), 33.51 (CH_2, 1C, C^{CS}).

*4.1.2.21. 4-(6-((4-(2-(ethylamino)pyrimidin-5-yl)benzyl)thio)pyridin-3-yl)benzaldehyde (**8c**).* ^{1}H NMR (400 MHz, DMSO-d_6) δ 10.06 (s, 1H, H^{CHO}), 8.92 (dd, J = 2.5, 1.0 Hz, 1H, H^{Py}), 8.59 (s, 2H, H^{Pym}), 8.08 (dd, J = 8.4, 2.5 Hz, 1H, H^{Py}), 8.01 (dt, J = 8.6, 2.1 Hz, 2H, H^{Ph}), 7.98 (dt, J = 8.6, 2.1 Hz, 2H, H^{Ph}), 7.56 (dt, J = 8.5, 2.1 Hz, 2H, H^{Ph}), 7.50 (dt, J = 8.5, 2.1 Hz, 2H, H^{Ph}), 7.47 (dd, J = 8.4, 0.9 Hz, 1H, H^{Py}), 7.29 (t, J = 5.7 Hz, 1H, H^{NH}), 4.52 (s, 2H, H^{CS}), 3.33 (qd, J = 7.1, 5.7 Hz, 2H, H^{NEt}), 1.13 (t, J = 7.1 Hz, 3H, H^{NEt}).

^{13}C NMR (101 MHz, DMSO-d_6) δ 193.21 (CH, 1C, C^{CHO}), 161.99 (C_q, 1C, C^{Pym}), 158.97 (C_q, 1C, C^{Py}), 156.23 (CH, 2C, C^{Pym}), 148.11 (CH, 1C, C^{Py}), 142.85 (C_q, 1C, C^{Ph}), 137.01 (C_q, 1C, C^{Ph}), 135.84 (C_q, 1C, C^{Ph}), 135.55 (CH, 1C, C^{Py}), 134.63 (C_q, 1C, C^{Pym}), 130.97 (C_q, 1C, C^{Py}), 130.72 (CH, 2C, C^{Ph}), 130.03 (CH, 2C, C^{Ph}), 127.60 (CH, 2C, C^{Ph}), 125.73 (CH, 2C, C^{Ph}), 122.18 (CH, 1C, C^{Py}), 121.82 (C_q, 1C, C^{Ph}), 35.94 (CH_2, 1C, C^{NEt}), 33.50 (CH_2, 1C, C^{CS}), 15.18 (CH_3, 1C, C^{NEt}).

*4.1.2.22. 4-(6-((4-(2-morpholinopyrimidin-5-yl)benzyl)thio)pyridin-3-yl)benzaldehyde (**8d**).* ^{1}H NMR (400 MHz, DMSO-d_6) δ 10.06 (s, 1H, H^{CHO}), 8.92 (d, J = 2.5 Hz, 1H, H^{Py}), 8.69 (s, 2H, H^{Pym}), 8.08 (dd, J = 8.4, 2.5 Hz, 1H, H^{Py}), 8.01 (d, J = 8.3 Hz, 2H, H^{Ph}), 7.98 (d, J = 8.3 Hz, 2H, H^{Ph}), 7.59 (d, J = 8.2 Hz, 2H, H^{Ph}), 7.51 (d, J = 8.2 Hz, 2H, H^{Ph}), 7.47 (d, J = 8.4 Hz, 1H, H^{Py}), 4.52 (s, 2H, H^{CS}), 3.77 (s, 4H, H^{Mpn}), 2.24 (s, 4H, H^{Mpn}).

^{1}H NMR (600 MHz, DMSO-d_6) δ 10.07 (s, 1H, H^{CHO}), 8.89 (d, J = 2.6 Hz, 1H, H^{Py}), 8.68 (s, 2H, H^{Pmy}), 8.04 (dd, J = 8.2, 2.6 Hz, 1H, H^{Py}), 8.00 (dt, J = 8.2, 2.2 Hz, 2H, H^{Ph}), 7.95 (d, J = 8.2 Hz, 2H, H^{Ph}), 7.58 (dt, J = 8.3, 2.4 Hz, 2H, H^{Ph}), 7.52 (d, J = 8.2 Hz, 1H, H^{Py}), 7.45 (d, J = 8.3 Hz, 2H, H^{Ph}), 4.53 (s, 2H, H^{CS}), 3.76 (t, J = 5.0 Hz, 4H, H^{Mpn}), 3.68 (t, J = 5.0 Hz, 4H, H^{Mpn}).

^{13}C NMR (151 MHz, DMSO-d_6) δ 192.11 (CH, 1C, C^{CHO}), 160.47 (C_q, 1C, C^{Pym}), 158.19 (C_q, 1C, C^{Py}), 155.29 (CH, 2C, C^{Pym}), 147.27 (CH, 1C, C^{Py}), 142.12 (C_q, 1C, C^{Ph}), 136.71 (C_q, 1C, C^{Ph}), 135.26 (C_q, 1C, C^{Ph}),

134.69 (CH, 1C, C^{Py}), 133.46 (C_q, 1C, C^{Pym}), 130.39 (C_q, 1C, C^{Py}), 129.83 (CH, 2C, C^{Ph}), 129.22 (CH, 2C, C^{Ph}), 126.79 (CH, 2C, C^{Ph}), 125.28 (CH, 2C, C^{Ph}), 121.85 (C_q, 1C, C^{Ph}), 121.49 (CH, 1C, C^{Py}), 65.68 (CH_2, 2C, C^{Mpn}), 43.89 (CH_2, 2C, C^{Mpn}), 33.03 (CH_2, 1C, C^{CS}).

*4.1.2.23. 4-(6-((4-(2-(4-methylpiperazin-1-yl)pyrimidin-5-yl)benzyl)thio) pyridin-3-yl)benzaldehyde (**8e**).* ^{1}H NMR (400 MHz, DMSO-d_6) δ 10.06 (s, 1H, H^{CHO}), 8.92 (d, J = 2.5 Hz, 1H, H^{Py}), 8.71 (s, 2H, H^{Pym}), 8.08 (dd, J = 8.6, 2.5 Hz, 1H, H^{Py}), 8.01 (d, J = 8.5 Hz, 2H, H^{Ph}), 7.98 (d, J = 8.5 Hz, 2H, H^{Ph}), 7.60 (d, J = 8.4 Hz, 2H, H^{Ph}), 7.52 (d, J = 8.4 Hz, 2H, H^{Ph}), 7.47 (d, J = 8.6 Hz, 1H, H^{Py}), 4.52 (s, 2H, H^{CS}), 3.74 (dt, J = 11.1, 4.2 Hz, 4H, H^{Ppn}), 3.65 (dt, J = 11.1, 4.2 Hz, 4H, H^{Ppn}), 1.27 (s, 3H, H^{NMe}).

^{1}H NMR (600 MHz, DMSO-d_6) δ 10.07 (s, 1H, H^{CHO}), 8.89 (d, J = 2.7 Hz, 1H, H^{Py}), 8.65 (s, 2H, H^{Pym}), 8.04 (dd, J = 8.3, 2.7 Hz, 1H, H^{Py}), 8.00 (d, J = 8.3 Hz, 2H, H^{Ph}), 7.95 (d, J = 8.3 Hz, 2H, H^{Ph}), 7.57 (d, J = 8.3 Hz, 2H, H^{Ph}), 7.51 (d, J = 8.3 Hz, 2H, H^{Ph}), 7.45 (d, J = 8.3 Hz, 1H, H^{Py}), 4.53 (s, 2H, H^{CS}), 3.79 (t, J = 5.1 Hz, 4H, H^{Ppz}), 2.41 (t, J = 5.1 Hz, 4H, H^{Ppz}), 2.25 (s, 3H, H^{NMe}).

^{13}C NMR (151 MHz, DMSO-d_6) δ 192.54 (CH, 1C, C^{CHO}), 160.85 (C_q, 1C, C^{Pym}), 158.65 (C_q, 1C, C^{Py}), 155.73 (CH, 2C, C^{Pym}), 147.72 (CH, 1C, C^{Py}), 142.57 (C_q, 1C, C^{Ph}), 137.07 (C_q, 1C, C^{Ph}), 135.72 (C_q, 1C, C^{Ph}), 135.13 (CH, 1C, C^{Py}), 134.00 (C_q, 1C, C^{Pym}), 130.84 (C_q, 1C, C^{Py}), 130.28 (CH, 2C, C^{Ph}), 129.65 (CH, 2C, C^{Ph}), 127.25 (CH, 2C, C^{Ph}), 125.67 (CH, 2C, C^{Ph}), 121.94 (CH, 1C, C^{Py}), 121.57 (C_q, 1C, C^{Ph}), 54.47 (CH_2, 2C, C^{Ppz}), 45.74 (CH_3, 1C, C^{NMe}), 43.61 (CH_2, 2C, C^{Ppz}), 33.49 (CH_2, 1C, C^{CS}).

*4.1.2.24. 4-(6-((4-(2-methoxypyrimidin-5-yl)benzyl)thio)pyridin-3-yl) benzaldehyde (**8f**).* ^{1}H NMR (400 MHz, DMSO-d_6) δ 10.06 (s, 1H, H^{CHO}), 8.92 (d, J = 2.5, 0.9 Hz, 1H, H^{CHO}), 8.92 (s, 2H, H^{Pym}), 8.08 (dd, J = 8.4, 2.5 Hz, 1H, H^{Py}), 8.01 (dt, J = 8.5, 2.2 Hz, 2H, H^{Ph}), 7.98 (dt, J = 8.5, 2.2 Hz, 2H, H^{Ph}), 7.68 (dt, J = 8.3, 2.1 Hz, 2H, H^{Ph}), 7.57 (dt, J = 8.3, 2.1 Hz, 2H, H^{Ph}), 7.48 (dd, J = 8.4, 0.9 Hz, 1H, H^{Py}), 4.55 (s, 2H, H^{CS}), 3.95 (s, 3H, H^{OMe}).

^{1}H NMR (600 MHz, DMSO-d_6) δ 10.07 (s, 1H, H^{CHO}), 8.89 (dd, J = 2.6, 0.9 Hz, 1H, H^{Py}), 8.87 (s, 2H, H^{Pym}), 8.04 (dd, J = 8.4, 2.6 Hz, 1H, H^{Py}), 8.01 (dt, J = 8.3, 2.0 Hz, 2H, H^{Ph}), 7.95 (dt, J = 8.2, 1.9 Hz, 2H, H^{Ph}), 7.66 (dt, J = 8.3, 2.0 Hz, 2H, H^{Ph}), 7.57 (dt, J = 8.2, 1.9 Hz, 2H, H^{Ph}), 7.46 (dd, J = 8.4, 0.9 Hz, 1H, H^{Py}), 4.55 (s, 2H, H^{CS}), 3.98 (s, 3H, H^{OMe}).

^{13}C NMR (151 MHz, DMSO-d_6) δ 192.12 (CH, 1C, C^{CHO}), 164.38 (C_q, 1C, C^{Pym}), 158.09 (C_q, 1C, C^{Py}), 156.80 (CH, 2C, C^{Pym}), 147.29 (CH, 1C, C^{Py}), 142.12 (C_q, 1C, C^{Ph}), 137.76 (C_q, 1C, C^{Ph}), 135.27 (C_q, 1C, C^{Ph}), 134.72 (CH, 1C, C^{Py}), 132.42 (C_q, 1C, C^{Ph}), 130.42 (C_q, 1C, C^{Py}), 129.84 (CH, 2C, C^{Ph}), 129.31 (CH, 2C, C^{Ph}), 126.89 (C_q, 1C, C^{Pym}), 126.81 (CH, 2C, C^{Ph}), 126.10 (CH, 2C, C^{Ph}), 121.52 (CH, 1C, C^{Py}), 54.30 (CH_3, 1C, C^{OMe}), 32.94 (CH_2, 1C, C^{CS}).

4.1.3. Products of reduction reaction

*4.1.3.1. (4-(1-methyl-1H-pyrazol-4-yl)phenyl)methanol (**2a**).* ^{1}H NMR (400 MHz, Chloroform-*d*) δ 7.76 (s, 1H, H^{Prz}), 7.61 (s, 1H, H^{Prz}), 7.47 (d, J = 8.2 Hz, 2H, H^{Ph}), 7.36 (d, J = 8.2 Hz, 2H, H^{Ph}), 4.69 (s, 2H, H^{CO}), 3.95 (s, 3H, H^{NMe}), 1.68 (s, 1H, H^{OH}).

^{13}C NMR (101 MHz, Chloroform-*d*) δ 139.08 (C_q, 1C, C^{Ph}), 136.92 (CH, 1C, C^{Prz}), 132.26 (C_q, 1C, C^{Ph}), 127.80 (CH, 2C, C^{Ph}), 127.07 (CH, 1C, C^{Prz}), 125.80 (CH, 2C, C^{Ph}), 123.06 (C_q, 1C, C^{Prz}), 65.34 (CH_2, 1C, C^{CO}), 39.25 (CH, 1C, C^{NMe}).

*4.1.3.2. (4-(1-benzyl-1H-pyrazol-4-yl)phenyl)methanol (**2b**).* ^{1}H NMR (400 MHz, Chloroform-*d*) δ 7.82 (s, 1H, H^{Prz}), 7.62 (s, 1H, H^{Prz}), 7.46 (dt, J = 8.1, 2.1 Hz, 2H, H^{Ph}), 7.35 (dt + m, J = 8.1, 2.1 Hz, 5H, $H^{Bz\ +\ Ph}$), 7.26 (dd, J = 7.5, 2.0 Hz, 2H, H^{Bz}), 5.34 (s, 2H, H^{Bz}), 4.68 (s, 2H, H^{CO}), 1.66 (s, 1H, H^{OH}).

^{13}C NMR (101 MHz, Chloroform-*d*) δ 139.13 (C_q, 1C, C^{Ph}), 137.17 (CH, 1C, C^{Prz}), 136.48 (C_q, 1C, C^{Bz}), 132.15 (C_q, 1C, C^{Ph}), 129.05 (CH, 2C, C^{Bz}), 128.34 (CH, 1C, C^{Bz}), 127.93 (CH, 1C, C^{Bz}), 127.75 (CH, 2C, C^{Ph}), 126.32 (CH, 1C, C^{Prz}), 125.80 (CH, 2C, C^{Ph}), 123.33 (C_q, 1C, C^{Prz}), 65.32 (CH_2, 1C, C^{CO}), 56.43 (CH_2, 1C, C^{Bz}).

*4.1.3.3. (4-(3,5-dimethylisoxazol-4-yl)phenyl)methanol (**2c**).* ^{1}H NMR (400 MHz, Chloroform-*d*) δ 7.45 (dt, J = 8.4, 2.0 Hz, 2H, H^{Ph}), 7.25 (dt, J = 8.4, 2.0 Hz, 2H, H^{Ph}), 4.75 (s, 2H, C^{CO}), 2.40 (s, 3H, H^{Me}), 2.27 (s, 3H, H^{Me}), 1.80 (s, 1H, C^{OH}).

^{13}C NMR (101 MHz, Chloroform-*d*) δ 165.40 (C_q, 1C, C^{Isx}), 158.85 (C_q, 1C, C^{Isx}), 140.31 (C_q, 1C, C^{Ph}), 129.96 (C_q, 1C, C^{Ph}), 129.42 (CH, 2C, C^{Ph}), 127.57 (CH, 2C, C^{Ph}), 116.52 (C_q, 1C, C^{Isx}), 65.13 (CH_2, 1C, C^{CO}), 11.69 (CH_3, 1C, C^{Me}), 10.93 (CH_3, 1C, C^{Me}).

*4.1.3.4. (3'-(dimethylamino)-[1,1'-biphenyl]-4-yl)methanol (**2e**).* ^{1}H NMR (400 MHz, Chloroform-*d*) δ 7.60 (dt, J = 8.4, 2.0 Hz, 2H, H^{Ph}), 7.43 (dt, J = 8.4, 2.0 Hz, 1H, H^{Ph}), 7.31 (dd, J = 8.3, 7.5 Hz, 1H), 6.94 (ddd, J = 7.5, 1.6, 0.9 Hz, 1H, H^{Ph}), 6.92 (dd, J = 2.6, 1.6 Hz, 1H, H^{Ph}), 6.75 (ddd, J = 8.3, 2.6, 0.9 Hz, 1H, H^{Ph}), 4.74 (d, J = 5.9 Hz, 2H, H^{CO}), 3.01 (s, 6H, H^{NMe}), 1.66 (t, J = 5.9 Hz, 1H, H^{OH}).

^{13}C NMR (101 MHz, Chloroform-*d*) δ 151.12 (C_q, 1C, C^{Ph}), 142.00 (C_q, 1C, C^{Ph}), 141.86 (C_q, 1C, C^{Ph}), 139.85 (C_q, 1C, C^{Ph}), 129.59 (CH, 1C, C^{Ph}), 127.67 (CH, 2C, C^{Ph}), 127.49 (CH, 2C, C^{Ph}), 115.91 (CH, 1C, C^{Ph}), 111.86 (CH, 1C, C^{Ph}), 111.62 (CH, 1C, C^{Ph}), 65.35 (CH, 1C, C^{CO}), 40.85 (CH, 2C, C^{NMe}).

*4.1.3.5. (4-(6-((4-(2-aminopyrimidin-5-yl)benzyl)thio)pyridin-3-yl) phenyl)methanol (**9a**).* ^{1}H NMR (400 MHz, DMSO-d_6) δ 8.80 (d, J = 2.5 Hz, 1H, H^{Py}), 8.55 (s, 2H, H^{Pym}), 7.96 (dd, J = 8.4, 2.5 Hz, 1H, H^{Py}), 7.68 (dt, J = , Hz, 2H, H^{Ph}), 7.56 (dt, J = , Hz, 2H, H^{Ph}), 7.49 (dt, J = , Hz, 2H, H^{Ph}), 7.43 (d, J = Hz, 2H, H^{Ph}), 7.40 (d, J = Hz, 1H, H^{Py}), 6.76 (s, 2H, H^{NH2}), 5.24 (t, J = 5.7 Hz, 1H, H^{OH}), 4.55 (d, J = 5.7 Hz, 2H, H^{CO}), 4.50 (s, 2H, H^{CS}).

^{13}C NMR (101 MHz, DMSO-d_6) δ 163.38 (C_q, 1C, C^{Pym}), 157.20 (C_q, 1C, C^{Py}), 156.33 (CH, 1C, C^{Pym}), 147.58 (CH, 1C, C^{Py}), 142.88 (C_q, 1C, C^{Ph}), 137.22 (C_q, 1C, C^{Ph}), 135.38 (C_q, 1C, C^{Ph}), 135.10 (CH, 1C, C^{Py}), 134.53 (C_q, 1C, C^{Pym}), 132.29 (C_q, 1C, C^{Ph}), 130.00 (CH, 2C, C^{Ph}), 127.64 (CH, 2C, C^{Ph}), 126.67 (CH, 2C, C^{Ph}), 125.75 (CH, 2C, C^{Ph}), 122.21 (C_q, 1C, C^{Py}), 122.13 (CH, 1C, C^{Py}), 63.02 (CH_2, 1C, C^{CO}), 33.53 (CH_2, 1C, C^{CS}).

HRMS (ESI): calcd for $C_{23}H_{20}N_4OS$ $[M + H]^+$, 400.1358; observed, 400.1358.

*4.1.3.6. (4-(6-((4-(2-(dimethylamino)pyrimidin-5-yl)benzyl)thio)pyridin-3-yl)phenyl)methanol (**9b**).* ^{1}H NMR (400 MHz, DMSO-d_6) δ 8.80 (dd, J = 2.5, 0.9 Hz, 1H, H^{Py}), 8.67 (s, 2H, H^{Pym}), 7.95 (dd, J = 8.5, 2.5 Hz, 1H, H^{Py}), 7.67 (dt, J = 8.4, 2.0 Hz, 2H, H^{Ph}), 7.57 (dt, J = 8.4, 2.0 Hz, 2H, H^{Ph}), 7.50 (dt, J = 8.4, 2.1 Hz, 2H, H^{Ph}), 7.43 (dt, J = 8.4, 2.1 Hz, 2H, H^{Ph}), 7.40 (dd, J = 8.5, 0.9 Hz, 1H, H^{Py}), 5.24 (t, J = 5.7 Hz, 1H, H^{OH}), 4.54 (d, J = 5.7 Hz, 2H, H^{CO}), 4.49 (s, 2H, H^{CS}), 3.15 (s, 6H, H^{NMe}).

^{13}C NMR (101 MHz, DMSO-d_6) δ 161.00 (C_q, 1C, C^{Pym}), 157.16 (C_q, 1C, C^{Py}), 156.16 (CH, 2C, C^{Pym}), 147.58 (CH, 1C, C^{Py}), 142.88 (C_q, 1C, C^{Ph}), 137.51 (C_q, 1C, C^{Ph}), 135.36 (C_q, 1C, C^{Ph}), 135.10 (CH, 1C, C^{Py}), 134.19 (C_q, 1C, C^{Ph}), 132.29 (C_q, 1C, C^{Py}), 130.03 (CH, 2C, C^{Ph}), 127.64 (CH, 2C, C^{Ph}), 126.67 (CH, 2C, C^{Ph}), 125.94 (CH, 2C, C^{Ph}), 122.14 (CH, 1C, C^{Py}), 122.08 (C_q, 1C, C^{Pym}), 63.01 (CH_2, 1C, C^{CO}), 37.21 (CH_3, 2C, C^{NMe}), 33.51 (CH_2, 1C, C^{CS}).

HRMS (ESI): calcd for $C_{25}H_{24}N_4OS$ $[M + H]^+$, 428.1671; observed, 428.1671.

*4.1.3.7. (4-(6-((4-(2-(ethylamino)pyrimidin-5-yl)benzyl)thio)pyridin-3-yl)phenyl)methanol (**9c**).* ^{1}H NMR (400 MHz, DMSO-d_6) δ 8.80 (dd, J = 2.5, 0.9 Hz, 1H, H^{Py}), 8.59 (s, 2H, H^{Pym}), 7.96 (dd, J = 8.4, 2.5 Hz, 1H, H^{Py}), 7.68 (dt, J = 8.3, 2.0 Hz, 2H, H^{Ph}), 7.56 (dt, J = 8.3, 2.0 Hz, 2H, H^{Ph}), 7.49 (dt, J = 8.4, 1.9 Hz, 2H, H^{Ph}), 7.43 (dt, J = 8.4, 1.9 Hz, 2H,

H^{Ph}), 7.40 (dd, J = 8.4, 0.9 Hz, 1H, H^{Py}), 7.29 (t, J = 5.7 Hz, 1H, H^{NH}), 5.24 (t, J = 5.6 Hz, 1H, H^{OH}), 4.55 (d, J = 5.6 Hz, 2H, H^{CO}), 4.50 (s, 2H, H^{CS}), 3.31 (q, J = 7.1 Hz, 2H, H^{NEt}), 1.14 (t, J = 7.1 Hz, 3H, H^{NEt}).

^{13}C NMR (101 MHz, DMSO-d_6) δ 161.99 (C_q, 1C, C^{Pym}), 157.07 (C_q, 1C, C^{Py}), 152.85 (CH, 2C, C^{Pym}), 147.67 (CH, 1C, C^{Py}), 144.00 (C_q, 1C, C^{Ph}), 138.47 (C_q, 1C, C^{Ph}), 136.79 (C_q, 1C, C^{Ph}), 136.11 (C_q, 1C, C^{Pym}), 135.26 (CH, 1C, C^{Py}), 132.58 (C_q, 1C, C^{Ph}), 130.67 (CH, 2C, C^{Ph}), 129.41 (CH, 2C, C^{Ph}), 125.31 (CH, 2C, C^{Ph}), 122.24 (CH, 1C, C^{Py}), 121.82 (C_q, 1C, C^{Py}), 119.65 (CH, 2C, C^{Ph}), 63.26 (CH_2, 1C, C^{CO}), 35.94 (CH_2, 1C, C^{NEt}), 33.17 (CH_2, 1C, C^{CS}), 15.18 (CH_3, 1C, C^{NEt}).

HRMS (ESI): calcd for $C_{25}H_{26}N_4OS$ [M + H]$^+$, 428.1671; observed, 428.1671.

*4.1.3.8. (4-(6-((4-(2-morpholinopyrimidin-5-yl)benzyl)thio)pyridin-3-yl) phenyl)methanol (**9d**).* ^{1}H NMR (400 MHz, DMSO-d_6) δ 8.81 (dd, J = 2.4, 0.9 Hz, 1H, H^{Py}), 8.72 (s, 2H, H^{Pym}), 7.96 (dd, J = 8.4, 2.4 Hz, 1H, H^{Py}), 7.68 (dt, J = 8.5, 2.1 Hz, 2H, H^{Ph}), 7.60 (dt, J = 8.5, 2.1 Hz, 2H, H^{Ph}), 7.52 (dt, J = 8.5, 2.1 Hz, 2H, H^{Ph}), 7.43 (dt, J = 8.5, 2.1 Hz, 2H, H^{Ph}), 7.40 (dd, J = 8.4, 0.9 Hz, 1H, H^{Py}), 5.24 (t, J = 5.7 Hz, 1H, H^{OH}), 4.55 (d, J = 5.7 Hz, 2H, H^{CO}), 4.51 (s, 2H, H^{CS}), 3.74 (td, J = 4.6, 1.5 Hz, 4H, H^{Mpn}), 3.68 (td, J = 4.6, 1.5 Hz, 4H, H^{Mpn}).

^{13}C NMR (101 MHz, DMSO-d_6) δ 161.08 (C_q, 1C, C^{Pym}), 157.15 (C_q, 1C, C^{Py}), 156.17 (CH, 2C, C^{Pym}), 147.58 (CH, 1C, C^{Py}), 142.88 (C_q, 1C, C^{Ph}), 137.62 (C_q, 1C, C^{Ph}), 135.36 (C_q, 1C, C^{Ph}), 135.10 (CH, 1C, C^{Py}), 134.09 (C_q, 1C, C^{Ph}), 132.29 (C_q, 1C, C^{Py}), 130.05 (CH, 2C, C^{Ph}), 127.64 (CH, 2C, C^{Ph}), 126.67 (CH, 2C, C^{Ph}), 126.01 (CH, 2C, C^{Ph}), 122.49 (C_q, 1C, C^{Pym}), 122.15 (CH, 1C, C^{Py}), 66.44 (CH_2, 2C, C^{Mpn}), 63.01 (CH_2, 1C, C^{CO}), 44.49 (CH_2, 2C, C^{Mpn}), 33.50 (CH_2, 1C, C^{CS}).

HRMS (ESI): calcd for $C_{27}H_{26}N_4O_2S$ [M + H]$^+$, 470.1776; observed, 470.1776.

*4.1.3.9. (4-(6-((4-(2-(4-methylpiperazin-1-yl)pyrimidin-5-yl)benzyl)thio) pyridin-3-yl)phenyl)methanol (**9e**).* ^{1}H NMR (400 MHz, DMSO-d_6) δ 8.81 (dd, J = 2.5, 0.9 Hz, 1H, H^{Py}), 8.69 (s, 2H, H^{Pym}), 7.96 (dd, J = 8.4, 2.5 Hz, 1H, H^{Py}), 7.68 (dt, J = 8.2, 2.1 Hz, 2H, H^{Ph}), 7.59 (dt, J = 8.5, 2.1 Hz, 2H, H^{Ph}), 7.51 (dt, J = 8.5, 2.1 Hz, 2H, H^{Ph}), 7.43 (dt, J = 8.2, 2.1 Hz, 2H, H^{Ph}), 7.40 (dd, J = 8.4, 0.9 Hz, 1H, H^{Py}), 5.24 (t, J = 5.8 Hz, 1H, H^{OH}), 4.55 (d, J = 5.8 Hz, 2H, H^{CO}), 4.50 (s, 2H, H^{CS}), 3.77 (t, J = 5.1 Hz, 4H, H^{Ppz}), 2.37 (t, J = 5.1 Hz, 4H, H^{Ppz}), 2.22 (s, 3H, H^{NMe}).

^{13}C NMR (101 MHz, DMSO-d_6) δ 161.00 (C_q, 1C, C^{Pym}), 157.16 (C_q, 1C, C^{Py}), 156.16 (CH, 2C, C^{Pym}), 147.58 (CH, 1C, C^{Py}), 142.88 (C_q, 1C, C^{Ph}), 137.51 (C_q, 1C, C^{Ph}), 135.36 (C_q, 1C, C^{Ph}), 135.10 (CH, 1C, C^{Py}), 134.19 (C_q, 1C, C^{Ph}), 132.29 (C_q, 1C, C^{Py}), 130.03 (CH, 2C, C^{Ph}), 127.64 (CH, 2C, C^{Ph}), 126.67 (CH, 2C, C^{Ph}), 125.94 (CH, 2C, C^{Ph}), 122.14 (CH, 1C, C^{Py}), 122.08 (C_q, 1C, C^{Pym}), 63.01 (CH_2, 1C, C^{CO}), 54.85 (CH_2, 2C, C^{Ppz}), 46.30 (CH_3, 1C, C^{NMe}), 43.89 (CH_2, 2C, C^{Ppz}), 33.51 (CH_2, 1C, C^{CS}).

HRMS (ESI): calcd for $C_{28}H_{29}N_3OS$ [M + H]$^+$, 483.2093; observed, 483.2093.

*4.1.3.10. (4-(6-((4-(2-methoxypyrimidin-5-yl)benzyl)thio)pyridin-3-yl) phenyl)methanol (**9f**).* ^{1}H NMR (400 MHz, DMSO-d_6) δ 8.92 (s, 2H, H^{Pym}), 8.81 (dd, J = 2.4, 0.9 Hz, 1H, H^{Py}), 7.96 (dd, J = 8.4, 2.4 Hz, 1H, H^{Py}), 7.68 (dt, J = 8.5, 2.1 Hz, 4H, H^{Ph}), 7.57 (dt, J = 8.5, 2.1 Hz, 2H, H^{Ph}), 7.43 (dt, J = 8.5, 2.1 Hz, 2H, H^{Ph}), 7.42 (dd, J = 8.4, 0.9 Hz, 1H, H^{Py}), 5.24 (t, J = 5.7 Hz, 1H, H^{OH}), 4.55 (d, J = 5.7 Hz, 2H, H^{CO}), 4.53 (s, 1H, H^{CS}), 3.96 (s, 3H, H^{OMe}).

^{13}C NMR (101 MHz, DMSO-d_6) δ 165.01 (C_q, 1C, C^{Pym}), 157.70 (CH, 2C, C^{Pym}), 157.05 (C_q, 1C, C^{Py}), 147.59 (CH, 1C, C^{Py}), 142.90 (C_q, 1C, C^{Ph}), 138.67 (C_q, 1C, C^{Ph}), 135.35 (C_q, 1C, C^{Ph}), 135.12 (CH, 1C, C^{Py}), 133.06 (C_q, 1C, C^{Ph}), 132.32 (C_q, 1C, C^{Py}), 130.13 (CH, 2C, C^{Ph}), 127.64 (CH, 2C, C^{Ph}), 127.57 (C_q, 1C, C^{Pym}), 126.86 (CH, 2C, C^{Ph}), 126.67 (CH, 2C, C^{Ph}), 122.17 (CH, 1C, C^{Py}), 63.01 (CH_2, 1C, C^{CO}), 55.19 (CH_3, 1C, C^{OMe}), 33.43 (CH_2, 1C, C^{CS}).

HRMS (ESI): calcd for $C_{24}H_{21}N_3O_2S$ [M + H]$^+$, 415.1354; observed, 415.1354.

4.1.4. Products of chlorination reaction

*4.1.4.1. 4-(4-(chloromethyl)phenyl)-1-methyl-1H-pyrazole (**3a**).* ^{1}H NMR (400 MHz, Chloroform-*d*) δ 7.76 (d, J = 0.9 Hz, 1H, H^{Prz}), 7.61 (d, J = 0.9 Hz, 1H, H^{Prz}), 7.45 (dt, J = 8.5, 2.0 Hz, 2H, H^{Ph}), 7.38 (dt, J = 8.5, 2.0 Hz, 2H, H^{Ph}), 4.59 (s, 2H, H^{CCl}), 3.94 (s, 3H, H^{NMe}).

^{13}C NMR (101 MHz, Chloroform-*d*) δ 136.92 (CH, 1C, C^{Prz}), 135.57 (C_q, 1C, C^{Ph}), 133.01 (C_q, 1C, C^{Ph}), 129.35 (CH, 2C, C^{Ph}), 127.19 (CH, 1C, C^{Prz}), 125.89 (CH, 2C, C^{Ph}), 122.77 (C_q, 1C, C^{Prz}), 46.32 (CH_2, 1C, C^{CCl}), 39.26 (CH, 1C, C^{NMe}).

*4.1.4.2. 1-benzyl-4-(4-(chloromethyl)phenyl)-1H-pyrazole (**3b**).* ^{1}H NMR (400 MHz, Chloroform-*d*) δ 7.83 (d, J = 0.9 Hz, 1H, H^{Prz}), 7.62 (d, J = 0.9 Hz, 1H, H^{Prz}), 7.45 (dt, J = 8.2, 2.0 Hz, 2H, H^{Ph}), 7.36 (dt + m, J = 8.2, 2.0 Hz, 5H, $H^{Bz\,+\,Ph}$), 7.27 (dd, J = 7.8, 1.9 Hz, 2H, H^{Bz}), 5.34 (s, 2H, H^{Bz}), 4.59 (s, 2H, H^{CCl}).

^{13}C NMR (101 MHz, Chloroform-*d*) δ 137.19 (CH, 1C, C^{Prz}), 136.41 (C_q, 1C, C^{Ph}), 135.62 (C_q, 1C, C^{Bz}), 132.92 (C_q, 1C, C^{Ph}), 129.31 (CH, 2C, C^{Ph}), 129.04 (CH, 2C, C^{Bz}), 128.34 (CH, 1C, C^{Bz}), 127.90 (CH, 2C, C^{Bz}), 126.44 (CH, 1C, C^{Prz}), 125.88 (CH, 2C, C^{Ph}), 123.04 (C_q, 1C, C^{Prz}), 56.42 (CH_2, 1C, C^{Bz}), 46.30 (CH_2, 1C, C^{CCl}).

*4.1.4.3. 4-(4-(chloromethyl)phenyl)-3,5-dimethylisoxazole (**3c**).* ^{1}H NMR (400 MHz, Chloroform-*d*) δ 7.46 (dt, J = 8.4, 2.0 Hz, 2H, H^{Ph}), 7.25 (dt, J = 8.4, 2.0 Hz, 2H, H^{Ph}), 4.63 (s, 2H, H^{CCl}), 2.41 (s, 3H, H^{Me}), 2.27 (s, 3H, H^{Me}).

^{13}C NMR (101 MHz, Chloroform-*d*) δ 165.56 (C_q, 1C, C^{Isx}), 158.75 (C_q, 1C, C^{Isx}), 136.89 (C_q, 1C, C^{Ph}), 130.83 (C_q, 1C, C^{Ph}), 129.54 (CH, 2C, C^{Ph}), 129.19 (CH, 2C, C^{Ph}), 116.25 (C_q, 1C, C^{Isx}), 45.98 (CH_2, 1C, C^{CCl}), 11.71 (CH_3, 1C, C^{Me}), 10.94 (CH_3, 1C, C^{Me}).

*4.1.4.4. 4'-(chloromethyl)-N,N-dimethyl-[1,1'-biphenyl]-3-amine (**3e**).* ^{1}H NMR (400 MHz, Chloroform-*d*) δ 7.59 (dt, 2H, H^{Ph}), 7.45 (dt, 2H, H^{Ph}), 7.31 (dd, J = 8.3, 7.5 Hz, 1H, H^{Ph}), 6.93 (ddd, J = 7.5, 1.7, 0.9 Hz, 1H, H^{Ph}), 6.90 (dd, J = 2.6, 1.7 Hz, 1H, H^{Ph}), 6.75 (dd, J = 2.6, 0.9 Hz, 1H, H^{Ph}), 4.64 (s, 2H, H^{CCl}), 3.01 (s, 6H, H^{NMe}).

^{13}C NMR (101 MHz, Chloroform-*d*) δ 151.11 (C_q, 1C, C^{Ph}), 142.63 (C_q, 1C, C^{Ph}), 141.71 (C_q, 1C, C^{Ph}), 136.40 (C_q, 1C, C^{Ph}), 129.63 (CH, 1C, C^{Ph}), 129.06 (CH, 2C, C^{Ph}), 127.84 (CH, 2C, C^{Ph}), 115.88 (CH, 1C, C^{Ph}), 112.00 (CH, 1C, C^{Ph}), 111.59 (CH, 1C, C^{Ph}), 46.30 (CH, 1C, C^{CCl}), 40.83 (CH, 2C, C^{NMe}).

4.1.5. Products of bimolecular nucleophilic substitution

*4.1.5.1. 5-bromo-2-((4-(1-methyl-1H-pyrazol-4-yl)benzyl)thio)pyridine (**4a**).* ^{1}H NMR (400 MHz, Chloroform-*d*) δ 8.51 (dd, J = 2.4, 0.8 Hz, 1H, H^{Py}), 7.73 (d, J = 0.9 Hz, 1H, H^{Prz}), 7.57 (d + dd, J = 8.5, 2.4, 0.9 Hz, 2H, $H^{Prz\,+\,Py}$), 7.39 (m, 4H, H^{Ph}), 7.06 (dd, J = 8.5, 0.8 Hz, 1H, H^{Py}), 4.40 (s, 2H, H^{CS}), 3.93 (s, 3H, H^{NMe}).

^{13}C NMR (101 MHz, Chloroform-*d*) δ 157.65 (C_q, 1C, C^{Py}), 150.36 (CH, 1C, C^{Py}), 138.66 (CH, 1C, C^{Py}), 136.90 (CH, 1C, C^{Prz}), 135.83 (C_q, 1C, C^{Ph}), 131.82 (C_q, 1C, C^{Ph}), 129.61 (CH, 2C, C^{Ph}), 127.00 (CH, 1C, C^{Prz}), 125.76 (CH, 2C, C^{Ph}), 123.39 (C_q, 1C, C^{Prz}), 123.04 (C_q, 1C, C^{Py}), 116.36 (CH, 1C, C^{Py}), 39.24 (CH, 1C, C^{NMe}), 34.53 (CH_2, 1C, C^{CS}).

*4.1.5.2. 2-((4-(1-benzyl-1H-pyrazol-4-yl)benzyl)thio)-5-bromopyridine (**4b**).* ^{1}H NMR (400 MHz, Chloroform-*d*) δ 8.50 (dd, J = 2.4, 0.8 Hz, 1H, H^{Py}), 7.79 (d, J = 0.9 Hz, 1H, H^{Prz}), 7.59 (d, J = 0.9 Hz, 1H, H^{Prz}), 7.56 (dd, J = 8.5, 2.4 Hz, 1H, H^{Py}), 7.37 (dt + dt + m, J = 8.6, 1.9 Hz, 7H, $H^{Bz\,+\,Ph}$), 7.24 (dd, J = 7.9, 1.6 Hz, 2H, H^{Bz}), 7.05 (dd, J = 8.5, 0.8 Hz, 1H, H^{Py}), 5.33 (s, 2H, H^{Bz}), 4.38 (s, 2H, H^{CS}).

^{13}C NMR (101 MHz, Chloroform-*d*) δ 157.63 (C_q, 1C, C^{Py}), 150.36 (CH, 1C, C^{Py}), 138.65 (CH, 1C, C^{Py}), 137.13 (CH, 1C, C^{Prz}), 136.50 (C_q,

1C, C^{Ph}), 135.89 (C_q, 1C, C^{Bz}), 131.69 (C_q, 1C, C^{Ph}), 129.61 (CH, 2C, C^{Ph}), 129.04 (CH, 2C, C^{Bz}), 128.32 (CH, 1C, C^{Bz}), 127.88 (CH, 2C, C^{Bz}), 126.30 (CH, 1C, C^{Prz}), 125.75 (CH, 2C, C^{Ph}), 123.40 (CH, 1C, C^{Py}), 123.31 (C_q, 1C, C^{Prz}), 116.36 (C_q, 1C, C^{Py}), 56.40 (CH_2, 1C, C^{Bz}), 34.54 (CH_2, 1C, C^{CS}).

*4.1.5.3. 4-(4-(((5-bromopyridin-2-yl)thio)methyl)phenyl)-3,5-dimethylisoxazole (**4c**).* ^{1}H NMR (400 MHz, Chloroform-*d*) δ 8.52 (dd, J = 2.4, 0.9 Hz, 1H, H^{Py}), 7.59 (dd, J = 8.5, 2.5 Hz, 1H, H^{Py}), 7.46 (dt, J = 8.2, 2.1 Hz, 2H, H^{Ph}), 7.18 (dt, J = 8.2, 2.1 Hz, 2H, H^{Ph}), 7.08 (dd, J = 8.5, 0.9 Hz, 1H, H^{Py}), 4.44 (s, 2H, H^{CS}), 2.39 (s, 3H, H^{Me}), 2.26 (s, 3H, H^{Me}).

^{13}C NMR (101 MHz, Chloroform-*d*) δ 165.38 (C_q, 1C, C^{Isx}), 158.83 (C_q, 1C, C^{Isx}), 157.37 (C_q, 1C, C^{Py}), 150.41 (CH, 1C, C^{Py}), 138.73 (CH, 1C, C^{Py}), 137.37 (C_q, 2C, C^{Ph}), 129.52 (CH, 2C, C^{Ph}), 129.32 (CH, 2C, C^{Ph}), 123.37 (CH, 1C, C^{Py}), 116.45 (C_q, 1C, C^{Isx}), 116.42 (C_q, 1C, C^{Py}), 34.24 (CH_2, 1C, C^{CS}), 11.75 (CH_3, 1C, C^{Me}), 10.99 (CH_3, 1C, C^{Me}).

*4.1.5.4. 4'-(((5-bromopyridin-2-yl)thio)methyl)-N,N-dimethyl-[1,1'-biphenyl]-3-amine (**4e**).* ^{1}H NMR (400 MHz, Chloroform-*d*) δ 8.52 (dd, J = 2.4, 0.8 Hz, 1H, H^{Py}), 7.58 (dd, J = 8.5, 2.4 Hz, 1H, H^{Py}), 7.52 (dt, J = 8.3, 2.0 Hz, 2H, H^{Ph}), 7.44 (dt, J = 8.3, 2.0 Hz, 2H, H^{Ph}), 7.29 (dd, J = 8.3, 7.5 Hz, 1H, H^{Ph}), 7.07 (dd, J = 8.5, 0.8 Hz, 1H, H^{Py}), 6.92 (ddd, J = 7.5, 1.9, 1.0 Hz, 1H, H^{Ph}), 6.89 (dd, J = 2.4, 1.9 Hz, 1H, H^{Ph}), 6.73 (ddd, J = 8.3, 2.4, 1.0 Hz, 1H, H^{Ph}), 4.44 (s, 2H, H^{CS}), 2.99 (s, 6H, H^{Ph}).

^{13}C NMR (101 MHz, Chloroform-*d*) δ 157.70 (C_q, 1C, C^{Py}), 151.08 (C_q, 1C, C^{Ph}), 150.38 (CH, 1C, C^{Py}), 141.96 (C_q, 1C, C^{Ph}), 141.39 (C_q, 1C, C^{Ph}), 138.67 (CH, 1C, C^{Py}), 136.65 (C_q, 1C, C^{Ph}), 129.55 (CH, 1C, C^{Ph}), 129.35 (CH, 2C, C^{Ph}), 127.61 (CH, 2C, C^{Ph}), 123.38 (CH, 1C, C^{Py}), 116.35 (C_q, 1C, C^{Py}), 115.87 (CH, 1C, C^{Ph}), 111.80 (CH, 1C, C^{Ph}), 111.59 (CH, 1C, C^{Ph}), 40.84 (CH, 1C, C^{CS}), 34.47 (CH, 2C, C^{NMe}).

*4.1.5.5. (Z)-2-((4-(1H-1,2,4-triazol-1-yl)benzyl)thio)-4-((1H-indol-3-yl)methylene)-1H-imidazole-5(4H)-one (**6**).* ^{1}H NMR (400 MHz, DMSO-d_6) δ 11.89 (t, J = 1.5 Hz, 1H, H^{NH}), 11.57 (s, 1H, H^{NH}), 9.25 (s, 1H, H^{Trz}), 8.45 (d, J = 2.6 Hz, 1H, H^{Vyn}), 8.21 (s, 1H, H^{Trz}), 8.13 (d, J = 8.0 Hz, 1H, H^{Ind}), 7.84 (dt, J = 8.5, 2.3 Hz, 2H, H^{Ph}), 7.73 (dt, J = 8.5, 2.3 Hz, 2H, H^{Ph}), 7.47 (dt, J = 8.0, 1.5 Hz, 1H, H^{Ind}), 7.20 (ddd, J = 8.0, 7.0, 1.2 Hz, 1H, H^{Ind}), 7.14 (ddd, J = 8.0, 7.0, 1.2 Hz, 1H, H^{Ind}), 7.13 (s, 1H, H^{Ind}), 4.67 (s, 2H, H^{CS}).

^{13}C NMR (101 MHz, DMSO-d_6) δ 170.50 (C_q, 1C, C^{Thd}), 158.57 (C_q, 1C, C^{Thd}), 152.90 (CH, 1C, C^{Trz}), 142.77 (CH, 1C, C^{Trz}), 137.89 (C_q, 1C, C^{Ph}), 136.81 (C_q, 1C, C^{Ind}), 136.38 (C_q, 1C, C^{Ph}), 135.23 (C_q, 1C, C^{Thd}), 132.57 (CH, 1C, C^{Vyn}), 130.79 (CH, 1C, C^{Ind}), 127.22 (C_q, 1C, C^{Ind}), 122.99 (CH, 1C, C^{Ind}), 121.14 (CH, 1C, C^{Ind}), 120.04 (CH, 2C, C^{Ph}), 120.01 (CH, 2C, C^{Ph}), 116.80 (CH, 1C, C^{Ind}), 112.66 (CH, 1C, C^{Ind}), 111.57 (C_q, 1C, C^{Ind}), 33.08 (CH_2, 1C, C^{CS}).

HRMS (ESI): calcd for $C_{21}H_{16}N_6OS$ $[M + H]^+$, 400.1106; observed, 400.1106.

4.2. Biology

4.2.1. Cells and viruses

RD cells (CCL-136) were provided by ATCC. They were cultivated in DMEM Media supplemented with 10 % fetal bovine serum (FBS), 1 % penicillin – streptomycin (PS), and 2 % non-essential amino acid. MRC-5 cells (CCL-171) were obtained from RD Biotech. They were cultivated in BME media supplemented with 10 % FBS, 1 % PS, and 1 % L-Glutamine. Both cell lines were grown at 37 °C in a 5 % CO_2 atmosphere.

EV A71 strain Laos2011 HFMD18TS (clinical strain), echovirus 30 strain UVE/E−30/2013/FR/4-MRS2013 and coxsackievirus A24 strain UVE/CV-A24/2010/LA/HFMK14St were provided through European Virus Archive – Global (respectively EVA – Global ***Ref-SKU:** 001v-EVA1553*, EVA – Global ***Ref-SKU:** 001v-EVA1517*, and EVA – Global ***Ref-SKU:** 001v-EVA1546*).

We selected these viruses to represent EV-A, EV-B, and EV-C species. EV-A and EV-B cause a variety of diseases, including hand-foot-mouth disease (HFMD) [1,36]. For instance, EVA-71, CV-A16, and E11 can be responsible for neurological symptoms, cardiopulmonary complications or acute hemorrhagic conjunctivitis in case of severe infections [37,38]. Likewise, acute flaccid paralysis, meningitis, or encephalitis can be caused by EV-B [4]. Finally, CVA24 has a variant that causes acute hemorrhagic conjunctivitis, a highly specific feature of this type of infection.

4.2.2. RNA extraction and quantification

Viral RNA was extracted from 100 µL of cell supernatant from passages P8 and P16 using a QIAamp Viral RNA kit on the automated QIAcube (Qiagen), according to the manufacturer's instructions. Relative quantification of viral RNA was performed using the GoTaq® 1-Step RT-qPCR System kit (Promega). The mixture contained 5 µL of 2x Master Mix, 0.25 µL of each primer (250 nM), 0.07 µL of probe (75 nM), 0.2 µL of GoScript RT Mix and 3.8 µL of extracted nucleic acids. For Enterovirus A, EV-A71F: AGATACCCACCCCCCTTACAA, EV-A71R: CACGTACGGGTGTTGCAACT, and EV-A71P FAM-CTCAACCCGGCGCC-MGB were used as primers and probes. For Enterovirus B and C, an already reported pan Enterovirus probe and primers were used [39]. Assays were performed using the QuantStudio 12 K Flex real-time PCR machine (Life technologies). Viral RNA was exposed at 50 °C for 15 min, then 95 °C for 2 min, followed by 40 cycles of 95 °C for 3 s, then 60 °C for 30 s. Data collection took place during the 60 °C step. Synthetic RNA was used to calculate the amount of viral RNA from standard curves.

4.2.3. EC_{50} and CC_{50} determination

One day prior to infection, 50000 RD cells, or 37500000 MRC-5 cells, per well were seeded in 100 µL assay medium containing 2.5 % FBS in 96-well culture plates. After 24 h exposure, antiviral compounds were added via the D300e dispenser (TECAN) with eight ½ dilutions. Then, 50 µL/well of a virus mix diluted in the medium was added to the wells. Each well was inoculated with XXX $TCID_{50}$ of the virus. Prior to the assay, it was verified that viruses in the cell culture supernatants were harvested during the logarithmic growth phase of viral replication at 72 h postinfection [40]. On each plate, Vapendavir (Medchemexpress) was used as a positive control at the same concentrations. Four virus control wells were included within the plate. On day 3 post-infection, the supernatant was harvested, and RNA was quantified as described above. Viral inhibition VI was calculated as follows:

$$VI = 100 \times \frac{(\overline{VC} - SQ)}{\overline{VC}}$$

with $\overline{VC}$ the mean quantity of viral control and SQ the sample quantity. The 50 % effective concentrations (EC_{50} compound concentration required to inhibit viral RNA replication by 50 %) and the 50 % cytotoxic concentration (CC_{50}) were determined by logarithmic interpolation after performing a nonlinear regression (log(inhibitor) vs. response–variable slope (three parameters)) as previously described [41]. All data obtained were analyzed using GraphPad Prism 9 software (GraphPad software).

4.2.4. Time-of-drug addition assays

For the TOA, we used the same experimental conditions as for the EC_{50} determination with the EV-A71 strain in RD cells. We used a non-cytotoxic concentration of HR-568 (10 µM). RD cell wells were treated 1 h before infection, at the time of infection, 2 h and 4 h post-infection. The viral supernatants were collected 72 h later and processed and analyzed as described above.

4.3. Docking

Docking calculations were performed on an Intel Xeon Silver-powered machine running Ubuntu 20.04 LTS. The X-ray crystal

structure of the EV-A71 capsid protein (PDB ID: 3ZFG) was initially prepared by reconstructing the missing loops and amino acid side chains. Subsequently, hydrogen atoms were added and minimized, fixing the positions of all heavy atoms until an RMSD gradient of 0.05 kcal mol^{-1} $Å^{-1}$ was reached. The 3D structures of the compounds were protonated at physiological pH and minimized using the OPLS4 force field [42]. The Maestro suite was used for both protein and ligand preparation steps [43]. PLANTS was utilized as the docking engine with default settings [44]. The geometrical center of the co-crystallized ligand was selected as the center of the docking sphere, with a radius of 12 Å. Molecular visualization and image processing were accomplished using PyMOL [45].

4.4. Evaluation of pharmacokinetic parameters

GastroPlus™ (Version 9.9; Simulations Plus, Inc., Lancaster, California, USA) software was used with a default parameter, namely the intake of a single tablet containing 100 mg of active compound, diluted in 250 mL of water, by a man on an empty stomach.

Only the bioavailability, the absorbed fraction, the log P, the molecular weight, the permeability, and the solubility were analyzed.

5. Conclusions

To obtain a broad-spectrum inhibitor of enteroviruses, we synthesized 21 thioether derivatives by optimized strategies and high yields.

The first series, containing **AB113** analogs, was developed to understand precisely each interaction between our compounds and the hydrophobic pocket. Unfortunately, except for **HR-267**, none of the derivatives were active anymore. Docking studies could explain this loss of activity by a steric hindrance with capsid amino acids.

In a second phase, fused bicycle derivatives were synthesized to combine **AB113** global structure with hydrophobic interactions of our previous series of **AB109** analogs. This time, according to docking studies, an extension of the *toe-end* side with this type of chemical structure should have favorable interactions. Among these derivatives, **OM1260** and **HR-568** inhibit EV-A71, from EV-A species, with micromolar potency (**OM1260**: EC_{50} (MRC-5, EV-A71) = 1.15 μM; EC_{50} (RD, EV-A71) = 4.38 μM; **HR-568**: EC_{50} (MRC-5, EV-A71) = 3.25 μM; EC_{50} (RD, EV-A71) = 1.53 μM). Admittedly, both derivatives are less effective than **AB113**, but with the great advantage of a broader spectrum. Indeed, both derivatives have micromolar activity against E30 and CVA24 virus, members respectively of the EV-B and the EV-C species (**OM1260**: EC_{50} (MRC-5, E30) = 0.41 μM; EC_{50} (MRC-5, CVA24) = 1.15 μM; **HR-568**: EC_{50} (MRC-5, E30) = 0.40 μM; EC_{50} (MRC-5, CVA24) = 1.22 μM). However, **OM1260** and **HR-568** have a lower selectivity index (SI between 7.1 and 17) than **AB113**. These could be an effect of the fused bicycles that are known to insert between the nucleic acid of DNA [46]. Works about substitutions to reduce cytotoxicity must be led, even if any aneugenic or clastogenic toxicity has been observed.

Eventually, these promising compounds possess sufficient bioavailability and associated permeability but poor solubility (<1 mg/L). A study about increasing solubility without reducing the activity has to be performed to come back to more favorable parameters.

CRediT authorship contribution statement

Hugo Roux: Writing – original draft, Investigation, Formal analysis, Data curation. **Franck Touret:** Writing – review & editing, Methodology, Investigation, Data curation. **Antonio Coluccia:** Writing – original draft, Methodology, Data curation. **Pietro Scio:** Software, Data curation. **Hawa Sophia Bouzidi:** Data curation. **Carole di Giorgio:** Data curation. **Florence Gattacceca:** Software. **Omar Khoumeri:** Data curation. **Romano Silvestri:** Supervision, Software. **Patrice Vanelle:** Writing – review & editing, Supervision. **Manon Roche:** Writing – review & editing, Validation, Supervision, Project administration, Methodology, Formal analysis, Conceptualization.

Associated content

(Word Style "TE_Supporting_Information"). Supporting Information. A brief statement in nonsentence format listing the contents of material supplied as Supporting Information should be included, ending with "This material is available free of charge via the Internet at http://pubs.acs.org." For instructions on what should be included in the Supporting Information as well as how to prepare this material for publication, refer to the journal's Instructions for Authors.

Funding sources

The authors declare no competing funding source.

Declaration of competing interest

The authors declare that they have no known competing financial interests or personal relationships that could have appeared to influence the work reported in this paper.

Acknowledgment

Aix Marseille Université (AMU) and the Centre National de la Recherche Scientifique (CNRS) are gratefully acknowledged for financial support. H. Roux thanks the Ministère de l'enseignement supérieur et de la recherche for his Ph.D. Grant. We thank Dr. Vincent Remusat for NMR analyses and Spectropole (Fédération des Sciences Chimiques de Marseille) for mass spectrometry, and complementary NMR analysis.

Appendix A. Supplementary data

Supplementary data to this article can be found online at https://doi.org/10.1016/j.ejmech.2025.117395.

Abbreviations

Multiplicity of NMR peak: d = doublet; dd = doublet of doublets; dt = doublet of triplets; ddd = doublet of doublet of doublets; m = multiplet; qd = quartet of doublets; t = triplet; td = triplet of doublets; s = singlet.

Chemical structures: Bzn, benzofurane; Idz, indazole; Ind, indole; Isq, isoquinoline; Nph, naphthalene; *N*-BzPrz, benzylpyrazole; *N*-MePrz, methylpyrazole; Ph, phenyl; Prz, pirazole; Py, pyridine; Thd, thiohydanthoin; Trz, triazole; 3-*N*dMeAni, 3-dimethylaniline; 4-*N*dMAni, 4-dimethylaniline; 3,5-dMeIsx, dimethylisoxazole.

Data availability

No data was used for the research described in the article.

References

[1] D.M. Brown, Y. Zhang, R.H. Scheuermann, Epidemiology and sequence-based evolutionary analysis of circulating non-polio enteroviruses, Microorganisms 8 (12) (2020) 1856, https://doi.org/10.3390/microorganisms8121856.
[2] T. Solomon, P. Lewthwaite, D. Perera, M.J. Cardosa, P. McMinn, M.H. Ooi, Virology, epidemiology, pathogenesis, and control of enterovirus 71, Lancet Infect. Dis. 10 (11) (2010) 778–790, https://doi.org/10.1016/S1473-3099(10)70194-8.
[3] D. Antona, M. Kossorotoff, I. Schuffenecker, A. Mirand, M. Leruez-Ville, C. Bassi, M. Aubart, F. Moulin, D. Lévy-Bruhl, C. Henquell, B. Lina, I. Desguerre, Severe paediatric conditions linked with EV-A71 and EV-D68, France, May to October 2016, Euro Surveill. 21 (46) (2016) 30402, https://doi.org/10.2807/1560-7917.ES.2016.21.46.30402.
[4] A. Fall, S. Kenmoe, J.T. Ebogo-Belobo, D.S. Mbaga, A. Bowo-Ngandji, J.R. Foe-Essomba, S. Tchatchouang, M. Amougou Atsama, J.F. Yéngué, R. Kenfack-Momo, A.F. Feudjio, A.D. Nka, C.A. Mbongue Mikangue, J.B. Taya-Fokou, J. N. Magoudjou-Pekam, E.A. Noura, C. Zemnou-Tepap, D. Meta-Djomsi, M. Maïdadi-

Foudi, G.I. Kame-Ngasse, I. Nyebe, L.G. Djukouo, L. Kengne Gounmadje, D. Tchami Ngongang, M.G. Oyono, C.P. Demeni Emoh, H.R. Tazokong, G. Mahamat, C. Kengne-Ndé, S.A. Sadeuh-Mba, N. Dia, G. La Rosa, L. Ndip, R. Njouom, Global prevalence and case fatality rate of Enterovirus D68 infections, a systematic review and meta-analysis, PLoS Neglected Trop. Dis. 16 (2) (2022) e0010073, https://doi.org/10.1371/journal.pntd.0010073.

[5] K.S. Benschop, J. Albert, A. Anton, C. Andrés, M. Aranzamendi, B. Armannsdóttir, J.L. Bailly, F. Baldanti, G.E. Baldvinsdóttir, S. Beard, N. Berginc, S. Böttcher, S. Blomqvist, L. Bubba, C. Calvo, M. Cabrerizo, A. Cavallero, C. Celma, F. Ceriotti, I. Costa, S. Cottrell, M. Del Cuerpo, J. Dean, J.L. Dembinski, S. Diedrich, J. Diez-Domingo, D. Dorenberg, E. Duizer, R. Dyrdak, D. Fanti, A. Farkas, S. Feeney, J. Flipse, C. De Gascun, C. Galli, I. Georgieva, L. Gifford, R. Guiomar, M. Hönemann, N. Ikonen, M. Jeannoël, L. Josset, K. Keeren, F.X. López-Labrador, M. Maier, J. McKenna, A. Meijer, B. Mengual-Chuliá, S.E. Midgley, A. Mirand, M. Montes, C. Moore, U. Morley, J.L. Murk, L. Nikolaeva-Glomb, S. Numanovic, M. Oggioni, P. Palminha, E. Pariani, L. Pellegrinelli, A. Piralla, C. Pietsch, L. Piñeiro, N. Rabella, P. Rainetova, S.C. Uceda Renteria, M.P. Romero, M. Reynders, L. Roorda, C. Savolainen-Kopra, I. Schuffenecker, A. Soynova, C. M. Swanink, T. Ursic, J.J. Verweij, J. Vila, T. Vuorinen, P. Simmonds, T.K. Fischer, H. Harvala, Re-emergence of enterovirus D68 in Europe after easing the COVID-19 lockdown, September 2021, Euro Surveill. 26 (45) (2021) 2100998, https://doi.org/10.2807/1560-7917.ES.2021.26.45.2100998.

[6] E.L. Forero, M. Knoester, L. Gard, A. Ott, A.H. Brandenburg, M.B.B. McCall, H.G. M. Niesters, C. Van Leer-Buter, Changes in enterovirus epidemiology after easing of lockdown measures, J. Clin. Virol. 169 (2023) 105617, https://doi.org/10.1016/j.jcv.2023.105617.

[7] H. Roux, F. Touret, A. Coluccia, O. Khoumeri, C. Di Giorgio, C. Majdi, P. Sciò, R. Silvestri, P. Vanelle, M. Roche, New potent EV-A71 antivirals targeting capsid, Eur. J. Med. Chem. 276 (2024) 116658, https://doi.org/10.1016/j.ejmech.2024.116658.

[8] M. Roche, C. Lacroix, O. Khoumeri, D. Franco, J. Neyts, T. Terme, P. Leyssen, P. Vanelle, Synthesis, biological activity and structure-activity relationship of 4,5-dimethoxybenzene derivatives inhibitor of rhinovirus 14 infection, Eur. J. Med. Chem. 76 (2014) 445–459, https://doi.org/10.1016/j.ejmech.2014.01.034.

[9] C. Lacroix, J. Querol-Audí, M. Roche, D. Franco, M. Froeyen, P. Guerra, T. Terme, P. Vanelle, N. Verdaguer, J. Neyts, P. Leyssen, A novel benzonitrile analogue inhibits rhinovirus replication, J. Antimicrob. Chemother. 69 (10) (2014) 2723–2732, https://doi.org/10.1093/jac/dku200.

[10] L. Da Costa, E. Scheers, A. Coluccia, A. Rosetti, M. Roche, J. Neyts, T. Terme, R. Cirilli, C. Mirabelli, R. Silvestri, P. Vanelle, Heterocyclic pharmacochemistry of new rhinovirus antiviral agents: a combined computational and experimental study, Eur. J. Med. Chem. 140 (2017) 528–541, https://doi.org/10.1016/j.ejmech.2017.09.036.

[11] L. Da Costa, E. Scheers, A. Coluccia, A. Casulli, M. Roche, C. Di Giorgio, J. Neyts, T. Terme, R. Cirilli, G. La Regina, R. Silvestri, C. Mirabelli, P. Vanelle, Structure-Based drug design of potent pyrazole derivatives against rhinovirus replication, J. Med. Chem. 61 (18) (2018) 8402–8416, https://doi.org/10.1021/acs.jmedchem.8b00931.

[12] L. Da Costa, M. Roche, E. Scheers, A. Coluccia, J. Neyts, T. Terme, P. Leyssen, R. Silvestri, P. Vanelle, VP1 crystal structure-guided exploration and optimization of 4,5-dimethoxybenzene-based inhibitors of rhinovirus 14 infection, Eur. J. Med. Chem. 115 (2016) 453–462, https://doi.org/10.1016/j.ejmech.2016.03.049.

[13] C. Tammaro, M. Guida, F. Appetecchia, M. Biava, S. Consalvi, G. Poce, Direct-acting antivirals and host-targeting approaches against enterovirus B infections: recent advances, Pharmaceuticals 16 (2) (2023) 203, https://doi.org/10.3390/ph16020203.

[14] J. Wang, Y. Hu, M. Zheng, Enterovirus A71 antivirals: past, present, and future, Acta Pharm. Sin. B 12 (4) (2022) 1542–1566, https://doi.org/10.1016/j.apsb.2021.08.017.

[15] Y. Hu, R. Musharrafieh, M. Zheng, J. Wang, Enterovirus D68 antivirals: past, present, and future, ACS Infect. Dis. 6 (7) (2020) 1572–1586, https://doi.org/10.1021/acsinfecdis.0c00120.

[16] J.Y. Lin, Y.A. Kung, S.R. Shih, Antivirals and vaccines for enterovirus A71, J. Biomed. Sci. 26 (1) (2019) 65, https://doi.org/10.1186/s12929-019-0560-7.

[17] S. Akkoç, Importance of some factors on the Suzuki-Miyaura cross-coupling reaction, J. Chin. Chem. Soc. 68 (6) (2021) 942–951, https://doi.org/10.1002/jccs.202000351.

[18] F. Touret, C. Baronti, O. Goethals, M. Van Loock, X. de Lamballerie, G. Querat, Phylogenetically based establishment of a dengue virus panel, representing all available genotypes, as a tool in dengue drug discovery, Antivir. Res. 168 (2019) 109–113, https://doi.org/10.1016/j.antiviral.2019.05.005.

[19] F. Touret, C. Baronti, O. Goethals, M. Van Loock, X. de Lamballerie, G. Querat, Phylogenetically based establishment of a dengue virus panel, representing all available genotypes, as a tool in dengue drug discovery, Antivir. Res. 168 (2019) 109–113, https://doi.org/10.1016/j.antiviral.2019.05.005.

[20] A. Tijsma, D. Franco, S. Tucker, R. Hilgenfeld, M. Froeyen, P. Leyssen, J. Neyts, The capsid binder Vapendavir and the novel protease inhibitor SG85 inhibit enterovirus 71 replication, Antimicrob. Agents Chemother. 58 (11) (2014) 6990–6992, https://doi.org/10.1128/AAC.03328-14.

[21] Y. Liu, Z. Zhang, X. Zhao, R. Yu, X. Zhang, S. Wu, J. Liu, X. Chi, X. Song, L. Fu, Y. Yu, L. Hou, W. Chen, Enterovirus 71 inhibits cellular type I interferon signaling by downregulating JAK1 protein expression, Viral Immunol. 27 (6) (2014) 267–276, https://doi.org/10.1089/vim.2013.0127.

[22] J.R. Wang, H.P. Tsai, S.W. Huang, P.H. Kuo, D. Kiang, C.C. Liu, Laboratory diagnosis and genetic analysis of an echovirus 30-associated outbreak of aseptic meningitis in Taiwan in 2001, J. Clin. Microbiol. 40 (12) (2002) 4439–4444, https://doi.org/10.1128/JCM.40.12.4439-4444.2002.

[23] K.C. Tsao, C.G. Huang, Y.L. Huang, F.C. Chen, P.N. Huang, Y.C. Huang, T.Y. Lin, S. R. Shih, S.C. Chang, Epidemiologic features and virus isolation of enteroviruses in Northern Taiwan during 2000-2008, J. Virol Methods 165 (2) (2010) 330–332, https://doi.org/10.1016/j.jviromet.2010.03.001.

[24] OCDE, Test No. 487: *in Vitro* Mammalian Cell Micronucleus Test, first ed., OCDE, Paris, 2010 https://doi.org/10.1787/9789264091016-en.

[25] K. Kobayashi, S. Koike, Adaptation and virulence of enterovirus-A71, Viruses 13 (8) (2021) 1661, https://doi.org/10.3390/v13081661.

[26] S. Tao, K. Zandi, L. Bassit, Y.T. Ong, K. Verma, P. Liu, J.A. Downs-Bowen, T. McBrayer, J.C. LeCher, J.J. Kohler, P.R. Tedbury, B. Kim, F. Amblard, S. G. Sarafianos, R.F. Schinazi, Comparison of anti-SARS-CoV-2 activity and intracellular metabolism of remdesivir and its parent nucleoside, Curr. Res. Pharmacol. Drug Discov. 2 (2021) 100045, https://doi.org/10.1016/j.crphar.2021.100045. Epub 2021 Aug 12. PMID: 34870151; PMCID: PMC8357487.

[27] C.Q. Sacramento, G.R. de Melo, C.S. de Freitas, N. Rocha, L.V. Hoelz, M. Miranda, N. Fintelman-Rodrigues, A. Marttorelli, A.C. Ferreira, G. Barbosa-Lima, J. L. Abrantes, Y.R. Vieira, M.M. Bastos, E. de Mello Volotão, E.P. Nunes, D. A. Tschoeke, L. Leomil, E.C. Loiola, P. Trindade, S.K. Rehen, F.A. Bozza, P.T. Bozza, N. Boechat, F.L. Thompson, A.M. de Filippis, K. Brüning, T.M. Souza, The clinically approved antiviral drug sofosbuvir inhibits Zika virus replication, Sci. Rep. 7 (2017 Jan 18) 40920, https://doi.org/10.1038/srep40920. Erratum in: Sci Rep. 2017 Apr 24;7:46772. doi: 10.1038/srep46772. PMID: 28098253; PMCID: PMC5241873.

[28] S. Tao, K. Zandi, L. Bassit, Y.T. Ong, K. Verma, P. Liu, J.A. Downs-Bowen, T. McBrayer, J.C. LeCher, J.J. Kohler, P.R. Tedbury, B. Kim, F. Amblard, S. G. Sarafianos, R.F. Schinazi, Comparison of anti-SARS-CoV-2 activity and intracellular metabolism of remdesivir and its parent nucleoside, Curr. Res. Pharmacol. Drug Discov. 2 (2021) 100045, https://doi.org/10.1016/j.crphar.2021.100045. Epub 2021 Aug 12. PMID: 34870151; PMCID: PMC8357487.

[29] a) C.Q. Sacramento, G.R. de Melo, C.S. de Freitas, N. Rocha, L.V. Hoelz, M. Miranda, N. Fintelman-Rodrigues, A. Marttorelli, A.C. Ferreira, G. Barbosa-Lima, J.L. Abrantes, Y.R. Vieira, M.M. Bastos, E. de Mello Volotão, E.P. Nunes, D. A. Tschoeke, L. Leomil, E.C. Loiola, P. Trindade, S.K. Rehen, F.A. Bozza, P.T. Bozza, N. Boechat, F.L. Thompson, A.M. de Filippis, K. Brüning, T.M. Souza, The clinically approved antiviral drug sofosbuvir inhibits Zika virus replication, Sci. Rep. 7 (2017 Jan 18) 40920, https://doi.org/10.1038/srep40920. Erratum in: Sci Rep. 2017 Apr 24;7:46772. doi: 10.1038/srep46772. PMID: 28098253; PMCID: PMC5241873; b) D.R. Owen, C.M.N. Allerton, A.S. Anderson, L. Aschenbrenner, M. Avery, S. Berritt, B. Boras, R.D. Cardin, A. Carlo, K.J. Coffman, A. Dantonio, L. Di, H. Eng, R. Ferre, K.S. Gajiwala, S.A. Gibson, S.E. Greasley, B.L. Hurst, E.P. Kadar, A. S. Kalgutkar, J.C. Lee, J. Lee, W. Liu, S.W. Mason, S. Noell, J.J. Novak, R.S. Obach, K. Ogilvie, N.C. Patel, M. Pettersson, D.K. Rai, M.R. Reese, M.F. Sammons, J. G. Sathish, R.S.P. Singh, C.M. Steppan, A.E. Stewart, J.B. Tuttle, L. Updyke, P. R. Verhoest, L. Wei, Q. Yang, Y. Zhu, An oral SARS-CoV-2 M^{pro} inhibitor clinical candidate for the treatment of COVID-19, Science 374 (6575) (2021 Dec 24) 1586–1593, https://doi.org/10.1126/science.abl4784. Epub 2021 Nov 2. PMID: 34726479.

[30] M.S. Oberste, S. Peñaranda, K. Maher, M.A. Pallansch, Complete genome sequences of all members of the species Human enterovirus A, J. Gen. Virol. 85 (Pt 6) (2004) 1597–1607, https://doi.org/10.1099/vir.0.79789-0.

[31] M.S. Oberste, K. Maher, M.A. Pallansch, Evidence for frequent recombination within species human enterovirus B based on complete genomic sequences of all thirty-seven serotypes, J. Virol. 78 (2) (2004) 855–867, https://doi.org/10.1128/jvi.78.2.855-867.2004.

[32] R.M. Ledford, N.R. Patel, T.M. Demenczuk, A. Watanyar, T. Herbertz, M.S. Collett, D.C. Pevear, P1 sequencing of all human rhinovirus serotypes: insights into genus phylogeny and susceptibility to antiviral capsid-binding compounds, J. Virol. 78 (7) (2004) 3663–3674, https://doi.org/10.1128/jvi.78.7.3663-3674.2004.

[33] Y.L. Huang, T.M. Lin, S.Y. Wang, J.R. Wang, The role of conserved arginine and proline residues in enterovirus VP1 protein, J. Microbiol. Immunol. Infect. 55 (4) (2022) 590–597, https://doi.org/10.1016/j.jmii.2022.01.004.

[34] J. Lu, Y.Q. He, L.N. Yi, H. Zan, H.F. Kung, M.L. He, Viral kinetics of enterovirus 71 in human abdomyosarcoma cells, World J. Gastroenterol. 17 (36) (2011) 4135–4142, https://doi.org/10.3748/wjg.v17.i36.4135.

[35] W.T. Jackson, T.H. Giddings Jr., M.P. Taylor, S. Mulinyawe, M. Rabinovitch, R. R. Kopito, K. Kirkegaard, PLoS Biol. 3 (5) (2005) e156, https://doi.org/10.1371/journal.pbio.00156.

[36] J.C. Haston, T.C. Dixon, Nonpolio enterovirus infections in neonates, Pediatr. Ann. 44 (5) (2015) e103–e107, https://doi.org/10.3928/00904481-20150512-09.

[37] L. Sun, A. Tijsma, C. Mirabelli, J. Baggen, M. Wahedi, D. Franco, A. De Palma, P. Leyssen, E. Verbeken, F.J.M. van Kuppeveld, J. Neyts, H.J. Thibaut, Intra-host emergence of an enterovirus A71 variant with enhanced PSGL1 usage and neurovirulence, Emerg. Microb. Infect. 8 (1) (2019) 1076–1085, https://doi.org/10.1080/22221751.2019.1644142.

[38] P.G. Higgins, Enteroviral conjunctivitis and its neurological complications, Arch. Virol. 73 (2) (1982) 91–101, https://doi.org/10.1007/BF01314718.

[39] T. Watkins-Riedel, M. Woegerbauer, D. Hollemann, P. Hufnagl, Rapid diagnosis of enterovirus infections by real-time PCR on the LightCycler using the TaqMan format, Diagn. Microbiol. Infect. Dis. 42 (2) (2002) 99–105, https://doi.org/10.1016/s0732-8893(01)00330-3.

[40] F. Touret, C. Baronti, O. Goethals, M. Van Loock, X. de Lamballerie, G. Querat, Phylogenetically based establishment of a dengue virus panel, representing all available genotypes, as a tool in dengue drug discovery, Antivir. Res. 168 (2019) 109–113, https://doi.org/10.1016/j.antiviral.2019.05.005.

[41] C. Lu, C. Wu, D. Ghoreishi, W. Chen, L. Wang, W. Damm, G.A. Ross, M.K. Dahlgren, E. Russell, C.D. Von Bargen, R. Abel, R.A. Friesner, E.D. Harder, OPLS4: improving force field accuracy on challenging regimes of chemical space, J. Chem. Theor. Comput. 17 (7) (2021) 4291–4300, https://doi.org/10.1021/acs.jctc.1c00302.
[42] Schrödinger Release 2024-2, Maestro, Schrödinger, LLC, New York, NY, 2024.
[43] O. Korb, T. Stützle, T.E. Exner, Empirical scoring functions for advanced protein-ligand docking with PLANTS, J. Chem. Inf. Model. 49 (1) (2009) 84–96, https://doi.org/10.1021/ci800298z.
[44] The PyMOL Molecular Graphics System, Version 3.0 Schrödinger, LLC.
[45] Sechi, M.; Derudas, M.; Dallochio, R.; Dessi, A.; Cosseddu, A.; Paglietti, G. DNA Binders:.
[46] Evaluation of DNA-interactive ability, design, and synthesis of novel intercalating agents, Lett. Drug Des. Discov. 6 (1) (2009) 56–62, https://doi.org/10.2174/157018009787158472.